energies

Review

Infrared Thermography in Photovoltaic Systems: A Review for Maximizing Energy Yield and Long-Term Reliability

Reza Sadeghi, Samuele Memme, Stefano Morchio, Marco Fossa * and Mattia Parenti

Dime Department of Mechanical, Energy, Management and Transportation Engineering, University of Genova, via Opera Pia 15a, 16145 Genova, Italy; reza.sadeghi@edu.unige.it (R.S.); samuele.memme@unige.it (S.M.); stefano.morchio@unige.it (S.M.); mattia.parenti@edu.unige.it (M.P.)

* Correspondence: marco.fossa@unige.it

Abstract

The growing deployment of photovoltaic (PV) systems worldwide has amplified the need for efficient, non-invasive diagnostic techniques to monitor their performance and ensure long-term reliability. Infrared (IR) thermography has emerged as a powerful tool for detecting thermal anomalies such as hotspots, cell mismatches, shading effects, and degradation in PV modules under real operating conditions. This review presents a comprehensive overview of recent advancements in thermographic analysis applied to PV diagnostics. It discusses the principles of thermal imaging, imaging protocols, and data interpretation techniques, alongside common thermal defects encountered in field and laboratory settings. Furthermore, the integration of irradiance mapping, drone-assisted surveys, and AI-based image analysis is examined for enhancing detection accuracy and scalability. The review also highlights standardization challenges, environmental influences, and emerging trends in automation and predictive maintenance. By consolidating current research, this study underscores the critical role of thermography in optimizing PV performance, reducing maintenance costs, and supporting the transition to smarter, more resilient solar energy infrastructures.

Keywords: thermography; photovoltaic; thermal anomalies; solar energy

1. Introduction

The global shift toward renewable energy sources has positioned solar photovoltaics (PV) at the core of decarbonization strategies, particularly within the European Union's roadmap toward climate neutrality. With global PV capacity now exceeding 1 TW, these systems are increasingly valued for their modularity, declining costs, and adaptability across residential, commercial, and utility-scale applications [1,2]. As outlined in the REPowerEU plan and the European Green Deal, photovoltaics are expected to play a leading role in achieving 2030 and 2050 climate targets. In parallel with Europe's decarbonization efforts, China has become the largest PV market worldwide, strongly influencing global solar deployment. By 2024, China's cumulative installed PV capacity exceeded 880 GW, with record annual additions of more than 270 GW, accounting for the majority of global new installations. Supported by national energy roadmaps extending toward 2030 and beyond, China is expected to maintain rapid PV expansion, reinforcing its role in achieving global climate targets alongside European initiatives. However, this rapid deployment also raises concerns about the long-term reliability and environmental impact of PV systems. Recent studies have emphasized the significance of reducing the carbon footprint of PV modules,

Academic Editors: Maciej Zajkowski, Adam Idzkowski and Stanislav Darula

Received: 6 February 2026
Revised: 12 March 2026
Accepted: 16 March 2026
Published: 23 March 2026

 https://doi.org/10.3390/en19061570

particularly during their manufacturing and transportation phases, which are identified as environmental hotspots within a cradle-to-gate lifecycle perspective [3]. At the operational level, PV modules remain susceptible to various degradation mechanisms and external stressors such as thermal cycling, humidity, soiling, shading, and mechanical stress that can lead to performance loss, hotspot formation, and accelerated aging [4,5]. Although PV technologies are generally regarded as durable, with manufacturer warranties extending up to 25 years, unmonitored failures can compromise safety and reduce energy yields. These challenges underline the need for advanced monitoring and fault detection techniques to ensure efficient maintenance, performance prediction, and lifecycle sustainability of solar assets [6].

To maintain the performance and safety of PV systems, accurate and timely diagnostic methods are essential. Conventional techniques such as I–V curve tracing, electroluminescence (EL), and photoluminescence (PL) imaging offer high precision but are often limited to laboratory settings or require system shutdowns [7,8]. In contrast, there is growing interest in fast, non-contact, and scalable inspection methods suitable for in-field conditions.

Infrared (IR) thermography is now routinely deployed as a powerful non-destructive diagnostic tool for detecting surface temperature variations in PV modules. By capturing thermal images under actual operating conditions, this technique enables rapid identification of localized anomalies such as hotspots, inactive cells, bypass diode failures, and interconnect issues [9,10]. The ability to visualize these defects in situ makes thermography particularly valuable for preventive maintenance and performance benchmarking in large PV installations [11]. IR thermography is mainly sensitive to temperature anomalies associated with localized heating. Therefore, degradation mechanisms and failures such as potential-induced degradation (PID), early-stage delamination, bypass diode malfunction under low or uniform current conditions, and homogeneous soiling may not produce detectable thermal signatures. As a result, these defects can be overlooked or ambiguously identified when IR thermography is used as a standalone diagnostic technique. In this sense, the IR thermography should be regarded as a complementary diagnostic tool rather than a standalone method.

Beyond PV diagnostics, IR thermography is also widely used in the building sector to visualize heat losses through façades and envelopes, supporting energy efficiency upgrades by identifying thermal bridges and poorly insulated areas. While many studies evaluate insulation, multilayer wall designs, shading, and thermal comfort mainly through simulation or conventional measurements [12–16], others directly combine these analyses with thermographic imaging to map surface temperature patterns and quantify envelope thermal performance under real operating conditions [17–20]. This broader application demonstrates the versatility of thermography as a contactless, field-deployable energy assessment tool. However, in contrast to building diagnostics, where steady-state heat transfer is predominant, the PV context involves dynamic electrical–thermal coupling under variable irradiance and environmental conditions, requiring a more specialized interpretation framework.

In PV systems, thermography must therefore be evaluated within a structured diagnostic perspective that considers three interrelated dimensions:

(i) Diagnostic performance, referring to detection accuracy, defect classification reliability, and sensitivity to early-stage degradation mechanisms;
(ii) Environmental influence, including irradiance variability, wind speed, viewing angle, emissivity uncertainty, and ambient temperature effects that can distort thermal signatures;
(iii) Economic impact, since early and accurate defect detection directly affects energy yield preservation, maintenance scheduling, and long-term system reliability.

Recent advancements in IR camera technology, combined with UAV (unmanned aerial vehicle) platforms, machine learning algorithms, and irradiance compensation techniques, have significantly extended the capabilities of thermographic inspections [21]. Artificial intelligence methods, including fuzzy logic, reinforcement learning, and real-time adaptive control, are increasingly being applied to enhance thermal diagnostics through intelligent interpretation of environmental and performance data [22]. In parallel, machine learning techniques such as deep learning and defect classification models are improving the accuracy and speed of fault detection in PV modules, especially for luminescence and thermographic imaging [23]. UAV-assisted thermography has demonstrated high effectiveness in detecting module-level defects based on temperature differentials, offering a scalable solution for rapid inspection of large PV fields [24].

These innovations enable high-resolution mapping, automated fault classification, and improved interpretation under varying environmental conditions. Nevertheless, challenges remain in standardizing inspection protocols, defining quantitative defect severity thresholds, and minimizing the influence of external factors such as wind speed and irradiance variability [25]. A critical evaluation of thermographic methodologies, classification schemes, and performance metrics within this diagnostic environmental economic framework is therefore essential to maximize energy yield and ensure long-term PV reliability, an objective that guides the structure of this review.

This review provides a comprehensive and up-to-date analysis of thermographic methods for photovoltaic (PV) diagnostics, covering foundational principles of thermal imaging, typical fault patterns, recent advances in data processing and automation, and practical applications across residential, commercial, and utility-scale PV systems. Particular emphasis is placed on infrared (IR) thermography as a rapid and scalable approach for fault detection, alongside the integration of artificial intelligence (AI), machine learning (ML), and unmanned aerial vehicles (UAVs) to enhance diagnostic accuracy, automation, and cost-effectiveness. By consolidating current knowledge and identifying research gaps, this work aims to advance thermography as a core strategy for intelligent PV monitoring and predictive maintenance.

1.1. Challenges in Operational Photovoltaic Systems

As the global demand for clean energy rises, PV systems have emerged as one of the most promising technologies for sustainable electricity generation. However, ensuring the long-term efficiency, safety, and economic viability of these systems requires reliable monitoring and maintenance approaches. In real-world conditions, PV modules are continuously exposed to a wide range of environmental and operational stressors that can lead to performance degradation and system failures. Despite their reputation for reliability and low maintenance, PV systems are not immune to faults, degradation, or external stress. A number of challenges affect both the performance and safety of PV farms, particularly as they scale in size and complexity [26]. One of the most common and critical issues is the formation of hotspots, where localized heating results from cell mismatch, shading, or internal defects [27]. Hotspots not only reduce energy output but can also accelerate module degradation and create fire risks if left undetected [28].

Additional challenges include potential-induced degradation (PID), microcracks, delamination, solder joint failures, and bypass diode malfunctions, all of which can impair module performance and contribute to uneven thermal behavior [7,26–28]. Soiling and shading are external factors that reduce irradiance on the module surface, often causing energy imbalances that may lead to thermal stress. Connector failures and junction box heating are less visible but pose significant safety hazards in aging systems [28,29].

1.2. Existing Diagnostic and Monitoring Methods

Various diagnostic tools and monitoring approaches have been developed to address faults in PV systems, each with distinct advantages and limitations. I–V curve tracing is widely used for electrical performance assessment but typically requires system downtime and skilled labor [30]. EL and PL imaging techniques are capable of detecting cell-level defects and microcracks with high accuracy, but they are generally confined to laboratory settings or require nighttime measurements, making them unsuitable for routine field inspections [31]. IR thermography is an inherently qualitative diagnostic technique, as it provides spatial information on surface temperature distributions without directly quantifying the impact of defects on the electrical performance parameters of photovoltaic modules. In contrast, I–V curve analysis and luminescence-based techniques, such as EL and PL, enable a quantitative assessment of defect severity and associated power losses. Consequently, defects such as PID, delamination, bypass diode malfunction, and soiling may be only partially or indirectly identified by IR thermography. For this reason, IR imaging is best employed as a screening tool to preselect modules for further investigation using I–V, EL, and/or PL techniques that provide quantitative performance information.

Field-level monitoring systems such as SCADA (Supervisory Control and Data Acquisition) and string-level inverters provide real-time electrical data but lack the spatial resolution to localize module-level faults [32]. Manual visual inspections, although cost-effective, are highly dependent on operator expertise and can miss hidden or internal issues. Furthermore, traditional inspection methods often involve reactive maintenance, identifying faults only after energy losses have occurred [27,30]. As PV installations become larger and more distributed, these conventional methods are increasingly insufficient for proactive and scalable maintenance strategies.

1.3. Thermographic Inspection as a Non-Invasive Solution

Infrared thermography is proven to be a promising solution for detecting surface temperature anomalies in PV modules under real operating conditions [26]. By capturing thermal images of PV surfaces, this method enables the rapid identification of localized heating patterns associated with common faults such as hotspots, defective bypass diodes, string mismatches, and soiling-related anomalies [33]. Recent advances in PV diagnostics have enabled non-contact and daylight operable variants of EL imaging, as well as concepts for non-contact I–V measurements, which can provide quantitative insights into module performance. Daylight EL (dEL) methodologies allow EL imaging under natural irradiance without module dismounting, using optical filtering and, in some implementations, self-powered configurations to inject current into the string, yielding defect images comparable to those obtained under traditional dark conditions, but with improved operational convenience for field inspection [34]. Luminescence-based techniques, including EL and PL, have been shown to correlate image intensity and patterns with electrical parameters such as power loss and cell degradation, enabling a more quantitative assessment of module health than surface temperature alone [35,36]. In contrast, IR thermography remains fundamentally qualitative: it detects temperature variations as proxies for electrical anomalies but does not directly quantify electrical parameters. While IR imaging under operational conditions can efficiently identify gross hotspots and surface thermal anomalies, it often lacks sensitivity to subtle or early-stage defects that do not produce significant thermal contrast. Therefore, IR thermography is best suited as a high-throughput screening technique to narrow down candidate modules for subsequent quantitative evaluation using I–V curve analysis and luminescence imaging, which provide higher resolution of internal defect structures and measurable impacts on electrical performance.

Thermal imaging is non-contact, does not require disconnection of modules, and can be performed in real time during normal operation [31,37]. Thermography is particularly well-suited for utility-scale PV farms, where the ability to scan hundreds or thousands of modules quickly is crucial [37,38]. The integration of thermal imaging with UAV platforms has further increased the feasibility and speed of large-scale inspections [39]. Additionally, with proper environmental corrections such as irradiance normalization and wind compensation [40], thermal inspections can offer reliable insights into PV system health and performance degradation. Despite some limitations, including sensitivity to environmental noise and the need for skilled interpretation, thermographic inspection represents a significant advancement in preventive maintenance for solar energy systems [7]. In summary, the IR thermography is a qualitative technique that:

- Detects surface temperature variations and hotspots.
- Conducts rapid, non-invasive screening of large arrays.
- Has limited sensitivity to early-stage or low-contrast defects.
- Cannot directly quantify electrical performance or power loss.

On the other hand, EL/PL is quantitative and:

- It provides high-resolution images of internal defect structures (cracks, shunts, PID, delamination).
- Intensity and pattern directly correlate with electrical parameters and power losses.
- Daylight EL (dEL) allows field inspection without module shutdown.
- It enables assessment of defect severity and degradation stage quantitatively.

The I–V Curve Analysis (quantitative):

- Measures module electrical performance directly under natural or controlled illumination.
- Detects current mismatch, bypass diode failures, and overall performance degradation.
- Demonstrates non-contact concepts for field measurements, though not yet fully commercialized.
- Provides quantitative metrics to evaluate impact of defects on output power and efficiency.

1.4. Research Scope and Contribution

This review advances the state of the art in photovoltaic (PV) diagnostics by redefining infrared thermography (IRT) as more than a conventional defect detection technique. Rather than treating thermography as an isolated inspection tool, the paper conceptualizes IRT as a scalable, intelligence-driven framework for performance optimization and long-term reliability management in PV systems. It should be noted that standalone IRTG is mainly qualitative. While it effectively localizes thermal anomalies, the interpretation of temperature patterns depends on environmental conditions and system-specific characteristics. Therefore, robust and generalizable modeling requires integration with electrical parameters, standardized acquisition protocols, or machine learning frameworks, and thermographic results should be interpreted as indicators rather than direct predictors of degradation mechanisms.

In contrast to previous reviews that primarily catalog degradation modes or focus on protocol-oriented imaging guidelines, this work systematically integrates thermographic fundamentals with UAV-assisted deployment strategies, irradiance-compensated analysis approaches, and emerging artificial intelligence methodologies for automated anomaly detection and predictive maintenance. By bridging methodological rigor with field-level scalability and smart operation and maintenance (O&M) strategies, the review positions thermography as a key enabling technology for next-generation, data-driven PV asset management and resilient solar energy infrastructures. The distinctive characteristics of the present contribution respect to the existent analyzed reviews are summarized in Table 1.

Table 1. Comparison of the present paper with other review papers in the literature.

Compared Document	Main Focus	Limitations	Distinctive Contribution of the Present Review
IEA, (2014) [8]	Comprehensive review of PV module failures	Foundational but descriptive; limited digitalization/automation perspective	Moves from descriptive failure cataloging to smart diagnostic integration and automation strategies
IEA, (2017) [41]	Field failure database and reliability statistics	Report-style, database-heavy, less innovation-driven	Adds forward-looking perspective: AI-driven automation, predictive maintenance, and intelligent image interpretation
IEA, (2018) [30]	IR and EL field imaging guidelines	Protocol- and standards-oriented; limited AI/automation integration	Extends beyond guidelines by integrating machine learning, UAV mapping, and intelligent fault classification
Kandeal et al., (2021) [10]	Infrared thermography for PV condition monitoring	Short, technique-centered, limited system integration and innovation scope	Provides broader integration of thermography + UAV + irradiance compensation + AI, moving beyond a mini-review into a strategic and scalable framework
Koester et al., (2022) [42]	Degradation mechanisms and techno-economic assessment	Focused on failure modes and cost evaluation rather than imaging methodology innovation	Positions thermography as an operational optimization tool, not only a defect indicator; emphasizes real-time monitoring and smart maintenance
IEA, (2023) [1]	Global PV market and policy trends	Market-focused; no diagnostic depth	Provides deep technical contribution directly linked to improving plant-level performance and resilience
Tardy, (2023) [20]	IR thermography for building envelope diagnostics	Not PV-specific; building-oriented	Strong PV-centered technical depth; links thermography directly to energy yield maximization and PV reliability
Michail et al., (2024) [33]	UAV-based imaging and fault detection	Broad UAV focus; less depth in thermographic physics and interpretation challenges	Combines methodological thermography analysis with UAV deployment, offering both technical rigor and scalability discussion
Del Prado Santamaría et al., (2025) [35]	Electroluminescence imaging and AI advancements	Technique-specific (EL only)	Focuses on thermal diagnostics under real operating conditions, offering practical field applicability without requiring system shutdown

The present document consolidates the current knowledge on:

a. The principles of thermographic imaging and best practices for field inspections.
b. The mapping of thermal patterns to specific PV fault types.
c. The role of UAVs in large-scale thermographic surveys.
d. The integration of AI and ML techniques for automated fault detection.
e. The challenges and limitations of current methods and prospects for standardization.

By synthesizing research across engineering, data science, and renewable energy domains, this paper aims to guide future innovation in intelligent PV monitoring systems, ultimately contributing to more resilient, efficient, and cost-effective solar energy infrastructures.

1.4.1. Annual Submissions of Publications on Infrared Thermography in PV Systems

A structured bibliometric analysis was conducted using the Web of Science Core Collection (WoSCC) database to evaluate the evolution of research on infrared thermography applied to photovoltaic (PV) systems over the period 2016–2025. The search was performed in January 2026 using a TAT (Title–Abstract–Topic) strategy, meaning that keywords were retrieved from the Topic (TS) field, which includes Title, Abstract, Author Keywords, and Keywords Plus. The Boolean search expression applied in the Web of Science Core Collection was: TS = ((“infrared thermography” AND “PV”) OR “photovoltaic thermography” OR “thermography using drone” OR “machine learning for PV fault detection” OR “thermal image processing on PV modules”).

The search was limited to the Web of Science Core Collection database. The Preprint Citation Index and Research Commons databases were excluded to ensure peer-reviewed content only. Furthermore, document types were restricted to Article and Review Article, while meeting abstracts, early access records, book chapters, editorial materials, data papers, clinical trials, and retracted publications were excluded to enhance dataset consistency and scientific reliability. Only English-language publications were considered.

After applying these filters and performing manual screening of titles and abstracts to remove unrelated applications (e.g., medical thermography or non-PV building studies), the final dataset consisted of 1438 publications.

Figure 1 illustrates the annual distribution of research output, where the vertical axis represents the number of publications and the horizontal axis denotes the publication year.

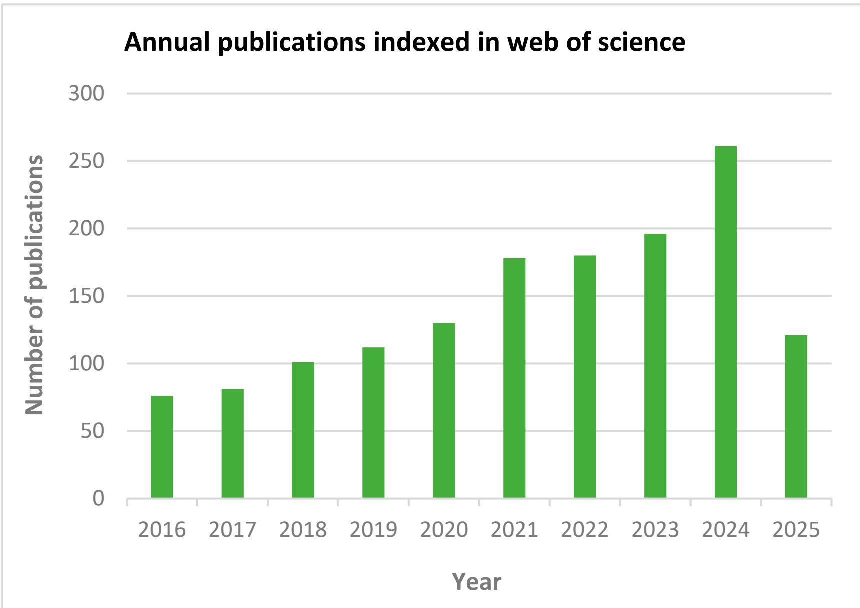

Figure 1. Annual publications indexed in the Web of Science Core Collection related to infrared thermography in PV systems, covering the period 2016–2025 (data for 2025 updated until September at the time of writing).

To provide analytical depth beyond publication counts, citation-based indicators (total citations and average citations per document) were extracted. In addition, keyword co-occurrence and thematic clustering analyses were performed using VOSviewer to identify dominant research themes and methodological trends within the field.

It should be noted that Web of Science subject categories are not mutually exclusive; a single publication may be classified under multiple subject areas (e.g., Energy and Fuels, Electrical Engineering, Materials Science). Therefore, the aggregated subject-area counts exceed the total number of unique publications, reflecting interdisciplinary overlap rather than inconsistency in the dataset.

The annual publication trend over the last decade shows a steady and sustained growth in research on infrared thermography in PV systems. Between 2016 and 2020, the increase was gradual, reflecting the consolidation of thermography as a practical diagnostic tool for hotspot detection and fault identification.

From 2021 onward, research output accelerated significantly, exceeding 170 publications annually. This growth coincides with the integration of UAV-based inspections, machine learning algorithms, and automated image-processing techniques for defect classification. The peak in 2024, with more than 250 indexed publications, indicates a strong expansion of research interest, driven by the convergence of thermographic diagnostics with intelligent data analysis and smart monitoring systems.

Although 2025 shows a lower count, this is due to partial database coverage at the time of data retrieval. Overall, the temporal evolution reflects not only quantitative growth but also a thematic shift toward automation, environmental compensation strategies, and performance-oriented diagnostic frameworks. These thematic patterns are further examined in the following subsections.

1.4.2. Geographical Distribution of Research Contributions

The geographical distribution of publications on infrared thermography in PV systems demonstrates active global engagement, with several countries emerging as key contributors. As presented in Figure 2, based on the analyzed Web of Science dataset, Germany leads with 293 records (16.32%), highlighting its strong research base in renewable energy diagnostics and performance monitoring. China follows with 251 publications (13.98%), underlining its rapid expansion in solar energy deployment and emphasis on advanced inspection technologies. The United States ranks third with 229 records (12.76%), reflecting its leadership in integrating UAV platforms, machine learning, and thermal imaging for PV fault detection.

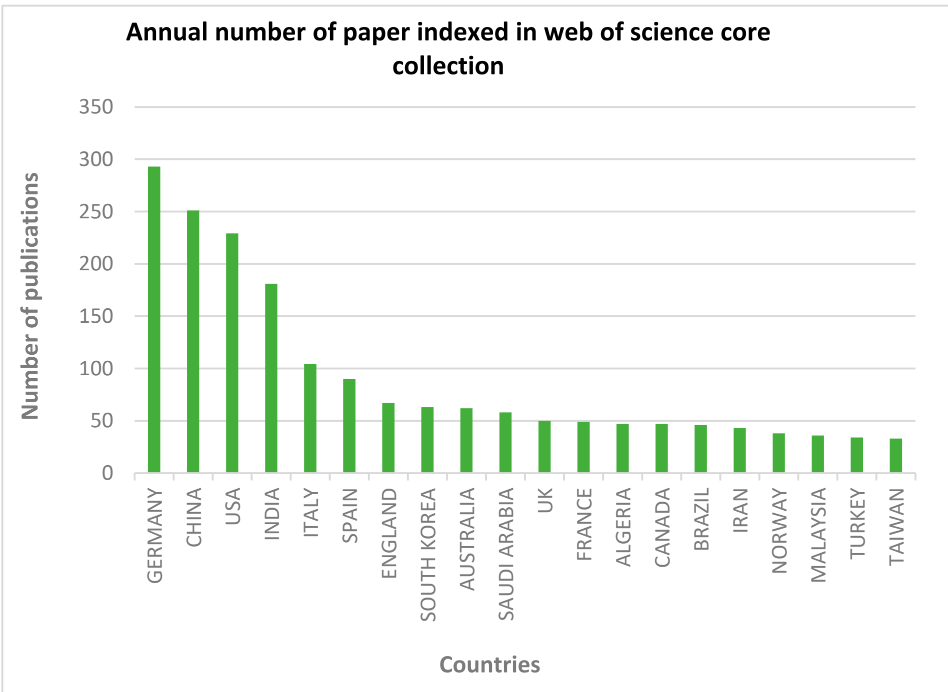

Figure 2. Geographical distribution of publications on infrared thermography in photovoltaic (PV) systems indexed in the Web of Science Core Collection, covering the period 2016–2025.

https://doi.org/10.3390/en19061570

India contributes 181 publications (10.08%), reflecting its large-scale solar initiatives, while Italy (104; 5.79%) and Spain (90; 5.01%) remain strong European contributors. England (67; 3.73%), South Korea (63; 3.51%), Australia (62; 3.45%), and Saudi Arabia (58; 3.23%) also demonstrate substantial research activity. Other countries including the UK, France, Algeria, Canada, and Brazil each account for more than 2% of total output, whereas Iran, Norway, Malaysia, Turkey, and Taiwan contribute smaller yet steadily increasing shares. Taken as a whole, this geographic spread indicates a broad and coordinated international effort, where both established research hubs and emerging regions are actively shaping the development of thermographic diagnostics for photovoltaic systems.

1.4.3. Publication Title Distribution

The distribution of research output across journals and conference proceedings is presented in Figure 3. The journal *Energies* leads with 69 publications (3.84%), reflecting its growing role as a platform for applied research in renewable energy diagnostics. Close behind are *Solar Energy* (67; 3.73%) and *Solar Energy Materials and Solar Cells* (67; 3.73%), both of which maintain strong traditions in advancing solar photovoltaic science and materials development. The *IEEE Journal of Photovoltaics* ranks fourth with 66 publications (3.68%), underscoring the importance of engineering-oriented approaches to PV performance and reliability. The *IEEE Photovoltaic Specialists Conference* contributes to 62 records (3.45%), highlighting the role of technical symposia in disseminating innovations in thermography and PV monitoring.

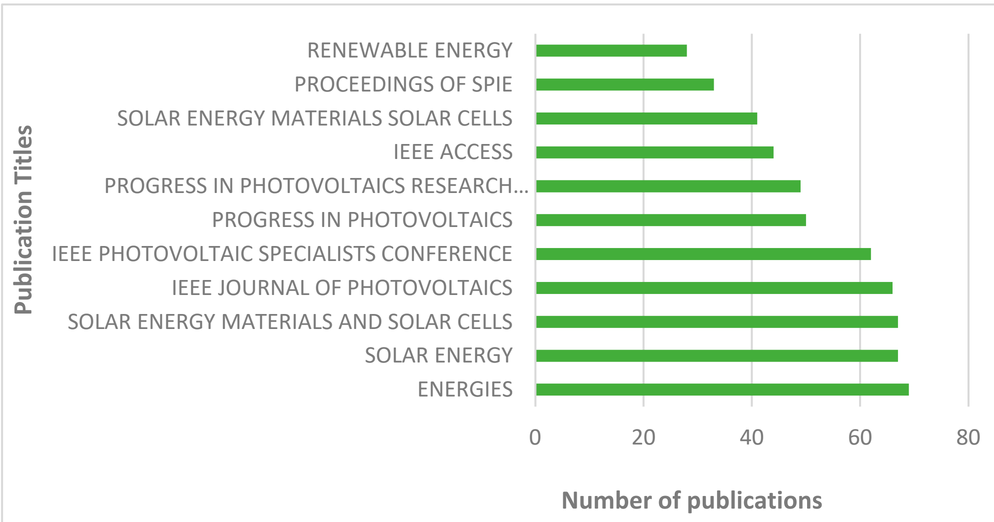

Figure 3. Distribution of publications on infrared thermography in PV systems by source titles indexed in the Web of Science Core Collection from 2016 to 2025.

Other influential sources include *Progress in Photovoltaics* (50; 2.79%) and *Progress in Photovoltaics: Research and Applications* (49; 2.73%), which together emphasize specialized advances in performance modeling and diagnostic methods. *IEEE Access* (44; 2.45%) provides an open-access platform for multidisciplinary contributions, while *Solar Energy Materials and Solar Cells* appears again under a separate indexing with 41 records (2.28%). Additionally, outlets such as *Proceedings of SPIE* (33; 1.84%) and *Renewable Energy* (28; 1.56%) reflect contributions from both conference-based and broader sustainability research. This distribution reflects the cross-disciplinary character of thermographic PV studies, spanning materials, diagnostics, and system-level applications.

1.4.4. Research Areas

The distribution of publications by research area is illustrated in Figure 4. The majority of contributions are concentrated in Engineering (1497 records; 83.40%) and Energy Fuels (1441; 80.28%), reflecting the strong technical and applied energy focus of thermography research in PV systems. Physics (727; 40.50%) and Materials Science (695; 38.72%) also represent substantial shares, underscoring the importance of fundamental principles and material related investigations in PV diagnostics.

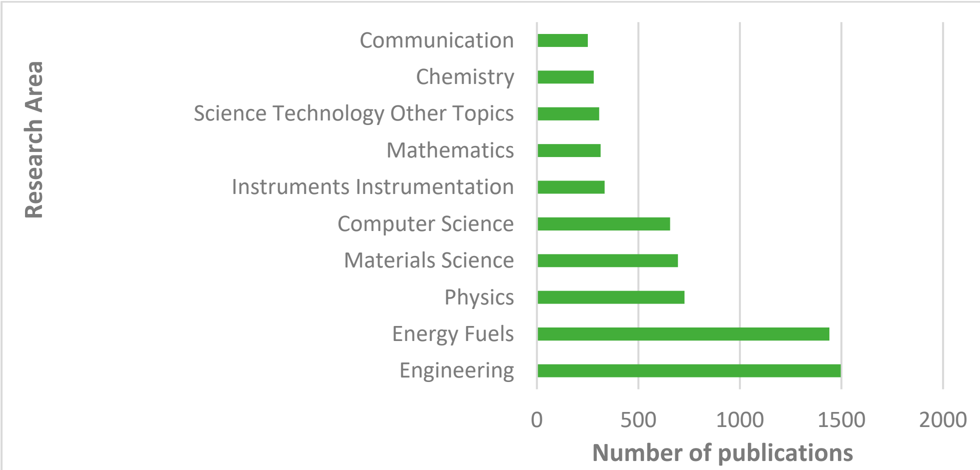

Figure 4. Distribution of publications on infrared thermography in PV systems by research area, based on records indexed in the Web of Science Core Collection from 2016 to 2025.

Additional significant areas include Computer Science (656; 36.55%), which highlights the growing role of artificial intelligence and machine learning in thermal image processing, and Instruments and Instrumentation (334; 18.61%), emphasizing the development of advanced imaging systems. Other contributions span Mathematics (314; 17.49%), Science and Technology Other Topics (307; 17.10%), Chemistry (280; 15.60%), and Communication (251; 13.98%). This broad distribution reflects the multidisciplinary nature of the field, where expertise in engineering, physics, computation, and applied sciences converges to advance reliable PV performance monitoring and predictive maintenance strategies.

2. Overview of Infrared Thermography

Thermography has become one of the most widely investigated non-destructive testing techniques (NDTTs) for PV diagnostics, primarily due to its ability to detect temperature anomalies without interrupting system operation. It operates based on detecting IR radiation naturally emitted by surfaces due to their thermal energy. Any object with a temperature above absolute zero emits IR radiation, which can be captured and analyzed using thermal imaging systems. When an external energy source, such as sunlight, strikes a surface, the energy is distributed in three main pathways: it can be reflected, absorbed, or transmitted, depending on the material's optical properties. The total incident irradiance (G) is the sum of the reflected (Gr), absorbed (Ga), and transmitted (Gt) components, i.e., $G = Gr + Ga + Gt$ [43]. For typical PV modules, the glass superstrate reflects only a small fraction of the incoming radiation at normal incidence (generally below ~6%), while the majority of the transmitted irradiance reaches the solar cells. The dominant heat generation mechanism occurs within the semiconductor material, where photons with energy exceeding the band gap undergo thermalization, and additional non-radiative recombination and resistive losses further contribute to temperature rise. The resulting heat is then conducted through the encapsulation layers toward the glass surface and dissipated to the environment by convection and infrared radiation. This energy conversion and heat transfer process explains why surface temperature patterns observed by infrared thermography primarily reflect internal electrical and material losses within the cells rather than direct heating of the glass itself. The schematic representation of the interactions among solar irradiance, atmosphere and a PV module is reported in Figure 5.

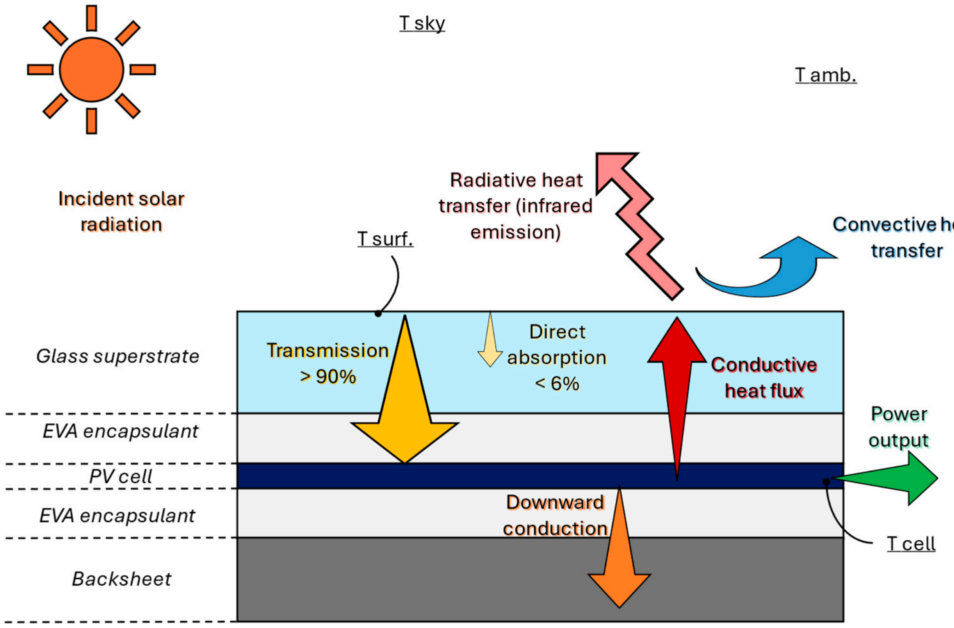

Figure 5. Schematic representation of solar irradiance interaction with a PV module, illustrating the different heat transfer mechanisms.

By capturing the infrared radiation emitted by objects, thermography allows for the visualization and analysis of surface temperature distributions, enabling the detection of defects such as hotspots, cracks, and delamination in PV modules without physical contact or system interruption. This section provides an overview of the fundamental concepts of thermography, its classifications, and the advanced methods developed for thermographic inspections in PV applications.

Recent advances in digital imaging have significantly simplified fault diagnostics in PV systems through the use of uncooled focal plane array detectors and charge coupled devices [44,45]. Among these, IRTG has demonstrated consistent effectiveness in not only fault detection but also precise localization of anomalies [41]. Electroluminescence (EL) imaging offers high accuracy for cell-level defects but faces practical limitations for outdoor inspections. IRTG provides a complementary non-contact method suitable for field applications, though its capabilities require clear de-lineation. IRTG effectively detects delamination, as the insulating air gap disrupts conductive heat flow from cells to the surface, creating detectable thermal patterns [46,47]. However, IRTG is not reliable for detecting structural defects in the glass superstrate: recent studies confirm that early-stage glass microcracks do not produce appreciable thermal signatures and are not identifiable through standard IRTG inspection [48]. It relies on thermal cameras to map temperature distributions across PV module surfaces, producing two- or three-dimensional pseudo-color images where healthy systems display homogeneous thermal patterns, and defective areas manifest as localized hotspots.

For reliable field inspections, IRTG measurements are typically performed under steady state illumination and stable weather conditions to ensure accurate readings. This capability makes IRTG especially attractive for predictive maintenance of PV systems [49], as it can be deployed without additional sensors or interruptions to normal operation. Recent years have seen a notable rise in publications applying IRTG to PV condition monitoring, reflecting its growing acceptance as a mainstream diagnostic tool. To better understand this trend, bibliometric mapping of keywords and co-occurrence networks has been carried out using VOSviewer software (https://www.vosviewer.com/, accessed on 2 October 2025), where node size reflects keyword frequency, link thickness indicates co-occurrence strength, and color shows publication year, revealing that IRTG has been increasingly applied in PV condition monitoring since 2016 [50]. A comparative experimental investigation highlighted those active thermographic approaches, such as step heating thermography (SHT), which not only confirm the presence of defective cells observed through passive imaging but can also accurately localize internal cracks within PV cells. These findings reinforce the potential of active thermography as a reliable nondestructive method for performance evaluation of PV modules, offering fast, intuitive, and reproducible results across various fault types [51].

The Infrared Thermography can be classified as in Figure 6, and the following paragraph contains a description of each category.

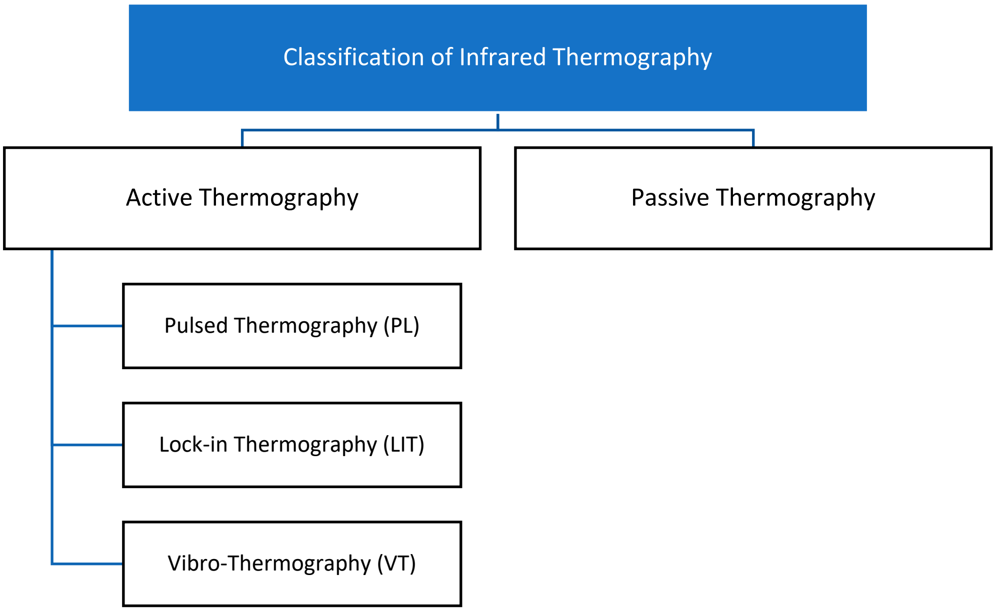

Figure 6. Classification of infrared thermography.

2.1. *Active Thermography in Photovoltaic Diagnostics*

Active thermography involves the deliberate application of external thermal excitation to PV surfaces to enhance the detection of subsurface anomalies. Unlike passive methods that rely solely on naturally emitted thermal radiation, active thermography uses controlled heating or cooling to induce a measurable thermal response. This approach is particularly effective in laboratory or indoor environments, where thermal inputs and ambient conditions can be tightly regulated. Three commonly used active thermographic techniques in PV diagnostics include pulsed thermography, lock-in thermography, and vibro-thermography.

Pulsed thermography involves applying a short burst of energy, typically from a flash lamp or halogen source to the PV module surface [52], followed by thermal imaging during the transient cooling phase. The resulting thermal gradient reveals subsurface anomalies due to localized heat accumulation, particularly in regions with delamination, cracks, or voids. However, the technique can be affected by non-uniform energy distribution and surface reflections, which can lead to a distortion of the image quality and require complex post processing algorithms for accurate defect interpretation [53].

Lock-in thermography (LIT) enhances thermal contrast by applying a periodic, modulated heat source, often a laser or halogen lamp, and synchronously capturing the thermal wave response: typical frequencies are around 10–40 Hz with thermal diffusion lengths of ~1.7 mm [54]. This phase sensitive detection technique is especially effective in identifying small-scale defects such as shunts, microcracks, and current leakage paths, making it widely used for quality control during PV cell manufacturing. Recent advancements have further extended the capabilities of LIT by introducing depth resolved analysis, which enables the differentiation of heat sources originating from the top, middle, or rear layers of the solar cell. These enhanced methods, such as the top-minus-bottom difference signal and imaginary Fast Fourier Transform (FFT) signal analysis, allow more precise localization of recombination regions and defects like backside contact failures or emitter surface scratches. Although challenges such as alignment artifacts and image noise remain, the results show that depth-resolved LIT can quantitatively identify vertical defect distributions, offering significant diagnostic potential beyond conventional surface-level inspections [54]; nonetheless, in UAV inspections of utility scale facilities, the required measurement conditions are difficult to replicate, contributing to diagnostic uncertainty.

Vibro-thermography utilizes ultrasonic excitation, typically in the range of 15–40 kHz, to induce localized frictional or strain-based heating at defect sites within the PV cell structure. The resulting transient thermal response is captured in real time using an infrared camera. This technique is particularly effective for detecting microcracks, delamination, and mechanical discontinuities in crystalline silicon wafers. Recent developments in resonance ultrasonic vibration (RUV) methods have further enhanced the efficiency of crack detection by exploiting frequency shifts and bandwidth changes in the vibrational response. Cracks cause a measurable decrease in wafer stiffness, leading to a downward shift in resonant frequency and broadening of the spectral peak. These changes correlate directly with crack length and severity, enabling both detection and preliminary defect characterization [55]. With data acquisition cycles as short as 2.4 s, including wafer loading, excitation, measurement, and release, the RUV-based vibro-thermography approach is highly compatible with high-throughput solar cell production lines. Overall, these active thermographic techniques, pulsed, lock-in, and vibro-thermography, offer complementary advantages for rapid, non-contact, and high-resolution fault detection in PV modules, supporting both quality control during manufacturing and predictive maintenance during operation. On the other hand, the remarkable disparity in inspection times highlights that there is no universal technique: while RUV takes few seconds per wafer and EL could take less than one second, high-resolution thermography (e.g., lock-in) takes minutes to hours, and UAV inspections on large plants take hours, depending on the scale.

2.2. Passive Thermography

Passive thermography involves monitoring PV modules under natural solar irradiance without external thermal stimulation. This approach relies on detecting surface temperature anomalies such as hotspots caused by defects like microcracks, delamination, or internal short circuits. Since the electrical performance of silicon-based modules is highly temperature sensitive, with power reductions of about 4–5% for a 10 °C increase in operating temperature, any localized heating pattern is often indicative of underlying faults that lead to efficiency losses [56]. IRTG, when passively applied under stable weather conditions, enables the identification of such faults in real time, making it suitable for large-scale outdoor inspections, especially when combined with UAVs.

Recent studies have advanced the field by quantifying the relationship between thermal anomalies and power losses on the system level. For instance, each module substring containing a thermal anomaly (false positives should be avoided considering only temperature differences higher than 5 °C) can reduce string output by an average of 1.16%, with more severe fault types contributing even greater losses [57]. However, the presence of multiple anomalies significantly correlates with cumulative energy degradation. Kandeal et al. [10] investigated the impact of the presence of thermal anomalies on the performance decay of a PV string with respect to fault free ones, analyzing thermographs and SCADA data from operating PV plants. In summary, localized overheating results in energy efficiency losses (at the string level) typically ranging from 2% to 4%, with some cases exceeding 5%. The most severe degradation occurs in modules affected by multiple hotspots or extended overtemperature conditions, while single hotspots or diode overheating exhibit more variable effects. Over time, thermal anomalies contribute to a progressive deterioration of performance, with an estimated annual degradation rate of up to 3%. These insights confirm that passive IRTG is not only a qualitative diagnostic tool but also valuable in performance prediction and targeted maintenance planning when combined with system-level analytics. Advanced techniques such as reverse bias thermography further enhance fault detection by accentuating heat dissipation at defect sites. Combined with scanning electron microscopy (SEM), researchers have linked hotspots to regions with high impurity concentrations, such as transition metals, which accelerate degradation mechanisms [58].

Field investigations, such as the study on the ETFOS 1 power plant, illustrate passive IRTG's practical utility. By analyzing 16 thermograms, researchers identified unexpected thermal patterns with temperature differentials ranging from 1.9 °C to 3.5 °C and emphasized the need for careful consideration of emissivity, reflection, and viewing angles: incorrect emissivity settings can introduce 2 °C errors, while glass reflection can cause up to 15 °C deviations depending on cloud cover. The study also highlighted the importance of operator training and standardized measurement protocols for accurate diagnostics [59].

Finally, both passive and active IRTG methods have proven effective for condition-based performance evaluation. In one study, passive IRTG successfully identified hotspots responsible for reduced output in underperforming modules. While limitations remain (such as environmental dependencies and material properties), passive IRTG stands out as a reliable, scalable solution for routine PV monitoring, offering real time diagnostics without interrupting system operation [60].

2.2.1. Effects of Camera–Module Alignment on Passive Thermography

The present authors conducted an experimental thermographic campaign on 10 July 2025 at the University of Genova Savona Campus, Savona, Italy, using a bifacial photovoltaic (BPV) solar bench equipped with a solar tracking system. The objective of this activity was to illustrate the influence of camera viewing geometry on the interpretation of passive infrared thermographic measurements under real outdoor operating conditions.

The thermographic measurements were performed using a FLIR T560 infrared camera (FLIR Systems, Wilsonville, OR, USA) mounted on a tripod to ensure stable acquisition conditions. The camera was positioned at a fixed distance of 6.00 m from the front surface of the PV module, with the lens located approximately at the same height as the module center. The BPV module was installed at a tilt angle $\beta = 35°$, while the camera viewing angle relative to the horizontal was $\theta_w = 55°$, as illustrated in Figure 7. During the campaign, the PV module was oriented at an azimuth angle of +60° (southwest).

Environmental conditions were monitored using pyranometers and an HT I–V curve tracer, allowing estimation of the plane of array irradiance during the thermographic sessions. Measurements were carried out at three representative times of the day, 09:45, 12:50, and 15:20, corresponding to morning, solar noon, and afternoon conditions. The recorded irradiance levels during these sessions were approximately 850 W m^{-2}, 1005 W m^{-2}, and 950 W m^{-2}, respectively. Figure 8 shows the experimental setup used during the campaign.

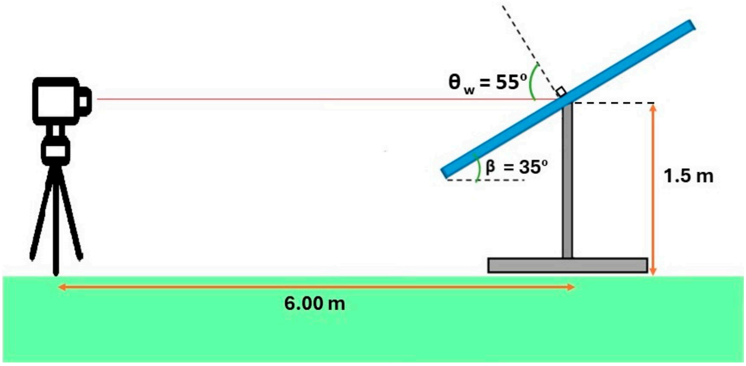

Figure 7. Schematic representation of the measurement geometry, indicating the PV module tilt angle (β = 35°) and the thermal camera viewing angle (θ_W = 55°) relative to the horizontal.

Figure 8. Experimental setup at the University of Genova Savona Campus showing the bifacial PV mobile bench oriented at an azimuth angle of +60° facing southwest, with the FLIR thermal camera mounted on a tripod at 6 m.

To evaluate the influence of viewing geometry on thermographic interpretation, the camera position was also varied by rotating it ±35° horizontally relative to the module central axis, while maintaining the same 6 m observation distance. These angular offsets, illustrated in Figure 9, represent eastward and westward viewing configurations and allow assessment of how off axis observation affects the apparent thermal distribution and hotspot visibility across the module surface. The three viewing angles (−35°, 0°, +35°) were acquired sequentially within a few minutes during each measurement session to ensure that ambient temperature and irradiance conditions remained approximately constant.

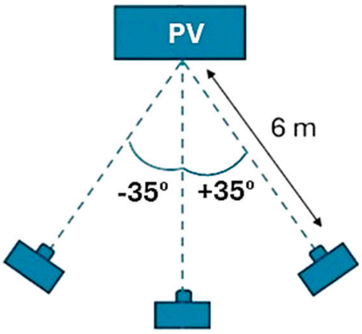

Figure 9. Schematic representation of horizontal camera angle variation (±35°) from the central axis of the PV module during thermographic inspection, while maintaining a constant distance of 6 m.

2.2.2. Results and Discussion

The thermographic observations summarized in Table 1 highlight the influence of irradiance level and viewing geometry on the apparent surface temperature distribution of the bifacial PV module.

During the morning session (09:45), the recorded plane of array irradiance was approximately 850 W m^{-2}. Under these conditions, the module exhibited relatively moderate surface temperatures with a fairly uniform distribution across the cells. Reference temperature measurements obtained from the electrical instrumentation indicated typical cell temperatures of approximately 48 °C for normal cells, while a deliberately perturbed cell (containing a small insulating element used to simulate a localized thermal disturbance) reached approximately 53 °C, illustrating the sensitivity of thermographic inspection to localized heating phenomena.

At solar noon (12:50), the irradiance increased to approximately 1005 W m^{-2}, leading to a noticeable increase in module temperature and a stronger thermal contrast in the thermograms. Under these conditions, the thermal distribution appeared more uniform across the module surface, and the influence of camera viewing angle was less pronounced because the module surface was more directly exposed to solar radiation.

During the afternoon measurement (15:20), irradiance levels remained relatively high (≈950 W m^{-2}), and the module continued to exhibit elevated surface temperatures. Because the solar azimuth at this time was closer to the module orientation (+60°), the panel maintained effective irradiance exposure despite the slightly lower global irradiance compared with noon conditions.

Comparison between the 0°, −35°, and +35° viewing configurations revealed that off-axis thermographic measurements can introduce variations in the apparent temperature field. These differences are mainly attributed to angular emissivity effects and reflection artifacts, which may slightly alter the perceived temperature gradients and hotspot visibility in infrared images. In contrast, near-normal viewing configurations tend to provide the most consistent representation of the emitted infrared radiation from the module surface. Although the measurements presented here correspond to a single illustrative field campaign, the observations highlight the practical importance of irradiance level, module orientation, and camera observation geometry in passive infrared thermography. Careful control of these parameters is therefore essential to ensure reliable interpretation of thermographic data during PV inspection campaigns.

3. Fault Types and Their Detectability Using Infrared Thermography

Understanding the types and implications of faults in PV systems is critical for ensuring both system safety and long-term performance reliability. Faults not only reduce the energy yield and operational efficiency of PV arrays but can also lead to premature degradation, posing safety risks such as fire hazards or electrical failure. These faults can range from chronic, high-risk issues such as line-to-line faults, ground faults, shading, and arc faults to more localized and less frequent problems like hotspots, bypass diode failures, or connection defects [60]. PV module failures are typically categorized into three temporal stages: infant failures (e.g., junction box defects, interconnection issues), midlife failures (e.g., delamination, glass breakage, or Ethylene Vinyl Acetate (EVA) discoloration), and wear-out failures (e.g., cell cracking, corrosion, or encapsulant degradation) [61]. Each type of fault can manifest distinct thermal or electrical signatures, impacting power output in varied ways depending on its location, severity, and interaction with environmental conditions [62]. Advancing diagnostic reliability requires not only identifying fault mechanisms and their root causes, but also addressing the practical limitations that hinder their early and accurate detection in real world conditions. In the following subsections, key PV fault types will be analyzed in detail to highlight their characteristics, detection methods, and implications for system performance and longevity.

3.1. Breakages and Cracks of PV Modules

Breakages and cracks are among the most frequent mechanical faults observed in PV modules and are critical to both performance degradation and long-term reliability. Glass breakage, in particular, is often introduced during transportation, installation, or maintenance activities and can lead to immediate or progressive damage in field conditions [63], and can also be induced by thermal shocks such as sudden cooling events [64]. Importantly, field observations indicate that glass breakage can create high-voltage safety hazards (e.g., insulation failure pathways and ground-fault risk) while the module may still deliver "useful power," meaning that damage may remain operationally masked until it escalates [63]. While some cracked or broken modules may initially continue functioning, their structural integrity is compromised, increasing susceptibility to moisture ingress, corrosion, delamination, and encapsulant discoloration over time [65]. In reliability/qualification contexts, mechanical stress tests are explicitly designed to trigger such damage mechanisms: for example, standardized static mechanical-load testing applies 2400 Pa (wind load) and up to 5400 Pa (snow load), while hail qualification uses a 25 mm ice ball at 23 m·s^{-1} at multiple impact locations [65], highlighting the stress magnitudes that can initiate glass/cell damage in practice: these can occur at loads as low as 2.4 kN under concentrated impact (e.g., hail or stepping) or 3300 Pa under uniform pressure [66]. An example of structural glass breakage caused by mounting stress is shown in Figure 10. Figure 11 illustrates typical crack propagation across solar cells within a module. Microcracks within cells, although not always visually detectable, disrupt current flow and lead to power losses, localized heating, and potential-induced degradation. Thermographically, damage-related heat-transfer disruption can amplify hotspot contrast: for instance, field-aged module observations report that delamination/packaging defects can contribute to a hotspot-to-background temperature difference exceeding ~30% by reducing local heat dissipation efficiency [63], which directly affects how anomalies appear in IRTG. EL imaging is widely recognized as the most effective technique for detecting minute defects such as microcracks in PV cells, which may not produce detectable thermal signatures in passive IRTG [67]. The importance of early microcrack detection is underscored by studies reporting potential long-term power losses of 5–30% [68]. Recent deep learning advances have significantly improved EL-based analysis: transformer-based models have achieved 83.40% recall and 86.20% precision on datasets comprising over 5000 annotated defects (70.9% linear microcracks) [68], while dual CNN architectures have reached 85.33% classification accuracy, reducing false negatives by 14% and false positives by 32% compared to conventional models [69]. Thus, EL imaging remains the gold standard for microcrack detection, complementing IRT which is better suited for identifying thermally active defects.

Figure 10. Example of glass breakage on a PV module caused by mechanical mounting stress (adapted from [70]).

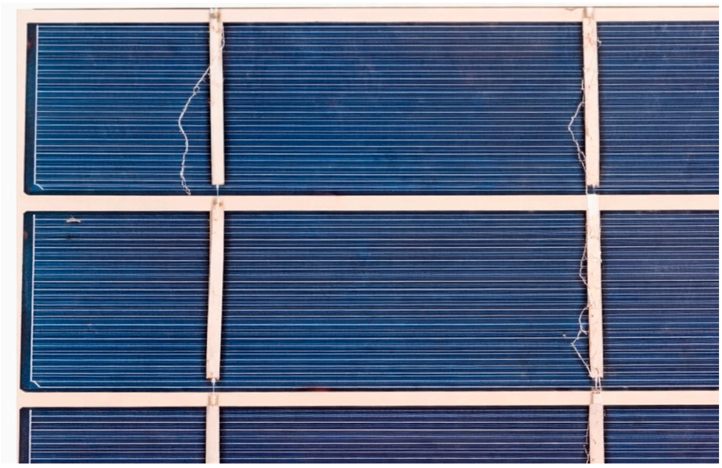

Figure 11. Crack propagation visible on the surface of PV cells, leading to localized electrical and thermal defects (adapted from [70]).

3.2. Delamination of PV Modules

Delamination refers to the loss of adhesion between the encapsulant and other layers of the PV module, such as the glass or the cells, and is a common degradation mechanism affecting long-term performance and safety. This phenomenon can increase optical reflection, reduce insulation, and allow moisture ingress, ultimately degrading the electrical performance of the module and accelerating corrosion processes [71]. Delamination is recognized as a significant reliability concern and is commonly evaluated through accelerated qualification tests. Standard IEC procedures include damp-heat exposure at 85 °C and 85% relative humidity for 1000 h, as well as humidity-freeze and UV-related stress tests designed to reveal adhesion loss and encapsulation degradation [63]. Although delamination does not immediately compromise safety, it can facilitate moisture ingress and create conductive paths that increase leakage currents and activate bypass diodes, leading to power losses. In such cases, infrared thermography becomes a valuable diagnostic tool, as it can reveal abnormal heat dissipation associated with increased series resistance or shunting effects. Furthermore, hotspot protection tests conducted under 1000 W m^{-2} irradiance, with exposure durations of 1–5 h depending on cell shunt resistance, highlight the stress conditions used to evaluate hotspot vulnerability when encapsulation integrity is compromised [63]. Delamination may indirectly contribute to thermally detectable anomalies by promoting moisture ingress and electrical degradation pathways such as shunting or increased series resistance, which can lead to localized heat dissipation detectable through infrared thermography [63].

As shown in Figure 12, delamination can appear as localized regions where the encapsulant layer separates from the underlying cell surface, often forming visible bubbles or cloudy areas within the module structure. Additionally, Figure 13 illustrates encapsulant separation from the glass near the busbars, made visible by the disruption of the glass texture: this often results from poor lamination or environmental stress. Manufacturing flaws such as improper lamination pressure, insufficient Ethylene Vinyl Acetate crosslinking, or contamination during production are common causes. However, external factors like thermal cycling, UV exposure, or mechanical stress also play significant roles. These defects are more severe in hot and humid environments and often serve as precursors to more critical issues like corrosion, insulation loss, or complete module failure.

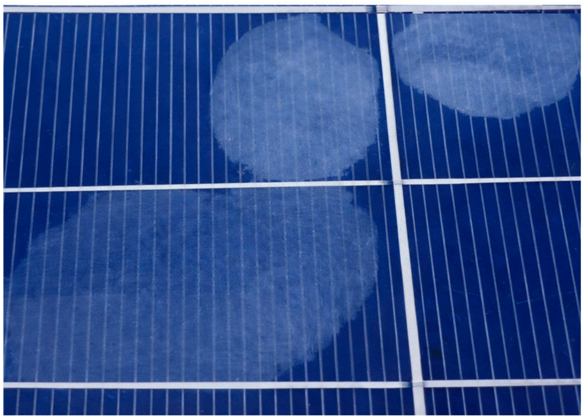

Figure 12. Example of delamination in a photovoltaic module, showing localized separation between the encapsulant and the solar cell surface, visible as cloudy regions within the cell area.

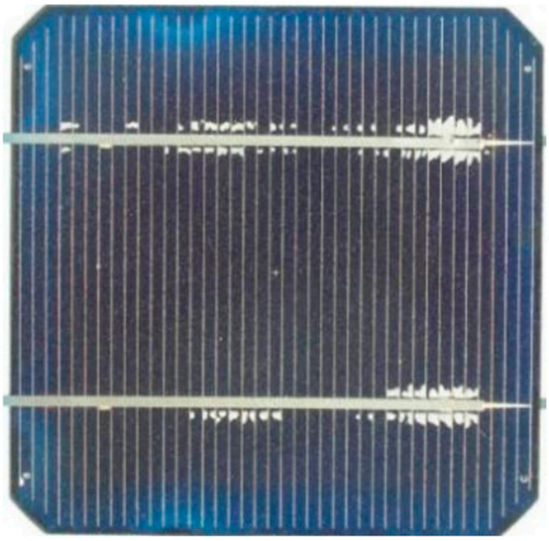

Figure 13. Encapsulant delamination from the glass along the busbars, identifiable through the disrupted glass texture [72].

3.3. Glass Corrosion or Abrasion in PV Modules

Glass corrosion or abrasion is a surface-level degradation commonly observed on the front layer of PV modules, manifesting as a cloudy, milky, or roughened appearance that reduces light transmittance. This effect is often the result of atmospheric interactions between moisture and pollutants such as salt, ammonia, or industrial emissions. In particular, dew can dissolve sodium ions from soda-lime glass, forming an alkali base that chemically attacks the silicate matrix [73]. Within large-scale failure surveys, corrosion or abrasion of anti-reflective (AR) coatings is classified as a distinct degradation mechanism. In such datasets, surface-related wear mechanisms—including AR coating degradation and glass surface damage—typically fall within lower annual degradation-rate intervals (commonly below 3% per year at system level), in contrast to electrically driven failures such as PIDs (≈15–16%/a) or defective bypass diodes (up to 25%/a in moderate climates). This quantitative contrast indicates that, while glass corrosion primarily affects optical transmission rather than electrical circuitry, its long-term cumulative impact can become relevant, particularly under aggressive environmental exposure.

The degradation can also stem from abrasive desert environments or improper cleaning practices, which strip or damage anti-reflective or anti-soiling coatings, thus diminishing optical performance and increasing susceptibility to further soiling. Though typically responsible for only a few percent of power loss annually, survey-based degradation classifications confirm that surface-related failures generally contribute lower annual degradation rates compared with cell cracks or PID mechanisms. Figure 14 illustrates a clear example of glass corrosion across a large module area, where the affected surface exhibits a widespread whitish haze that severely limits light penetration and may progressively reduce energy yield over time.

Figure 14. Advanced glass corrosion across a PV module surface, showing widespread hazing and opacity caused by environmental exposure. The affected area exhibits reduced transparency and transmission loss, likely due to degradation of anti-reflective coatings and chemical interactions with atmospheric pollutants [74].

3.4. Metallisation, Discolouration and Corrosion

In addition to glass surface degradation, corrosion and discolouration of the cell metallisation and interconnect ribbons represent another prevalent fault type in PV modules. This defect typically appears as yellow, brown, or even black discoloration of the solder bonds, gridlines, fingers, or ribbons, and may be accompanied by powdery or colored galvanic products depending on the materials used. Unlike glass corrosion, which affects optical transmission, metallisation corrosion primarily impacts electrical performance by increasing series resistance, thereby reducing module output. Quantitative field studies confirm this progression: modules affected solely by encapsulant discoloration exhibit median power losses of 4–5% over 20+ years [75]. Figure 15 illustrates two cases of metallisation-related damage: the left image shows discolouration of the ribbon due to corrosion, while the right image captures string interconnect corrosion along the busbars, both of which are potential sources of mismatch and performance degradation.

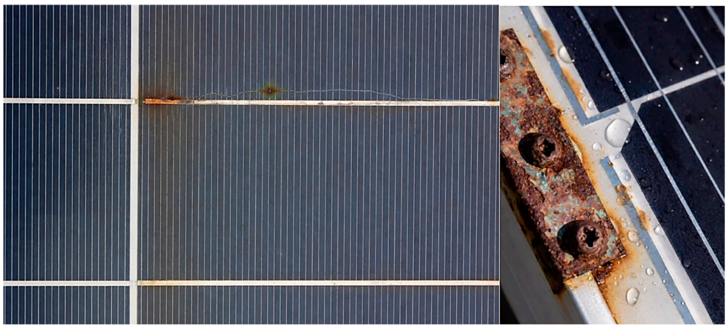

Figure 15. (**Left**) Discolouration of the ribbon due to corrosion along the interconnects. (**Right**) Corrosion of the string interconnect ribbon near the busbar, showing early-stage oxidation and degradation effects.

This degradation mode is commonly caused by the presence of acetic acid, a byproduct of Ethylene Vinyl Acetate (EVA) encapsulant degradation in the presence of moisture and oxygen, often following delamination. Poor soldering quality, improper lamination times, or low-resistance materials such as tin-coated copper can further exacerbate the issue. Environmental conditions like high humidity, agricultural or maritime exposure, and temperature fluctuations significantly increase the corrosion risk: in moderate climates, metallization corrosion affects ~20–25% of modules after 11–20 years and ~30–35% after 20+ years, while in hot–humid climates, the fraction exceeds 40% in older installations [75]. While metallisation discolouration alone may not present an immediate safety hazard, it can lead to increased mismatch losses and bypass diode activation, especially when combined with other failure modes such as delamination or encapsulant browning.

3.5. Hotspots and Strings

Hotspots are localized thermal anomalies caused by defects such as cell cracks, shading, or interconnect failures that drive affected cells into reverse bias [76–78], causing them to dissipate energy as heat. Under reverse-bias conditions, localized avalanche breakdown may occur, and focal-point heating can exceed 150 °C, a temperature above the critical stability limit of common encapsulants, thereby accelerating delamination and insulation failure. Experimental investigations show that under reverse bias (≈ -10 V and 3 A), severely affected cells can develop temperature peaks approaching 150 °C, while even moderate reverse dissipation (~11 W) can generate temperature gradients of $\approx$25 K across a single cell [79]. These elevated temperatures accelerate material degradation and pose long-term reliability and safety concerns.

IRTG is widely applied in field inspections to detect such faults quickly and non-invasively, particularly when thermal contrasts reveal early-stage reverse-bias heating before catastrophic burnout occurs. To mitigate hotspot risks, it is recommended that the number of cells per sub-string be limited to 18–20 cells, as reverse-bias voltage increases proportionally with series length. Analytical modeling shows that for a typical 18-cell sub-string protected by a bypass diode, the maximum reverse bias may reach approximately -10 V, while extending to 24 cells may fail to provide sufficient protection in several tested cell types. Therefore, enhanced reverse-bias testing protocols during module qualification, as suggested in [79], are essential to identify worst-case cells and prevent irreversible hotspot damage during operation.

Further investigations into hotspot sensitivity have shown that both crystalline and amorphous silicon modules are vulnerable to localized heating under reverse-bias conditions. According to [80], intrusive and non-intrusive experiments revealed that in commercial amorphous silicon modules, localized damage typically occurs at the interconnections between cells when the reverse-bias current density exceeds 5–20 mA/cm^2. Interestingly, while current mismatch is a known contributor to hotspots, shading was found to cause even greater temperature rise, making it a more critical factor in field conditions, and the research is contributing to the modules' orientation optimization to reduce shading losses in both fixed [81] and tracking systems [82]. For the tested monolithic amorphous silicon modules, despite substantial current mismatch between individual cells, the observed temperature rise was minimal due to their inherently low shunt resistance. As a consequence, the hotspot severity and the thermal resilience of PV modules under stress conditions are dependent on the module design characteristics such as interconnection configuration and shunt resistance.

While hotspots are not always directly visible, their thermal effects are critical in identifying hidden PV module issues. They are characterized by localized overheating or irregular thermal patterns that can only be reliably detected via imaging techniques such as infrared thermography. Although mild temperature gradients (<10 K) are typically benign, gradients exceeding 20 K may indicate serious failures or even safety risks. As shown in Table 2, the nature and severity of hotspots depend on factors such as shading, poor soldering, cell mismatch, delamination, or potential-induced degradation (PID). These defects can force cells into reverse bias, causing them to dissipate power as heat. If left unaddressed, this can lead to burn marks, encapsulant damage, glass breakage, or even fire hazards. Importantly, not all hotspots immediately lead to power loss: modules with a single hot cell may still operate within acceptable performance margins. However, when bypass diodes are permanently activated due to fault severity, power losses can escalate significantly across strings or entire arrays. In particular, long-term operation without maintenance (e.g., cleaning of soiling or bird droppings) can mask evolving hotspot damage. Therefore, detecting the thermal pattern early allows preventative actions before irreversible damage occurs. The patterns presented in Table 3 highlight common fault modes and their corresponding performance impacts, serving as diagnostic tools for system operators.

As summarized in Table 3, thermal imaging helps classify hotspot patterns by linking them to specific electrical and physical faults. Open-circuit faults appear as warmer but mostly functional modules, while short-circuits or bypass diode failures cause localized heating and power loss. More severe issues like PID or polarization result in broader heating near frames, requiring corrective action. Other issues, such as shadowing, delamination, or bird droppings, create distinct asymmetrical or sharp hotspots. Identifying these patterns is key to effective fault diagnosis and system reliability. Infrared thermography under reverse-bias conditions was employed by Simon and Meyer [58] to investigate the origin and effects of hotspot formation in crystalline silicon solar cells. The study used infrared thermography under reverse-bias conditions to investigate hotspot formation in c-Si solar cells. Localized heating was observed, with temperatures rising from 80 °C to 150 °C over one hour. Scanning electron microscopy (SEM) analysis revealed irreversible structural damage at hotspot sites, including surface deformation. Energy-dispersive X-ray spectroscopy (EDX) and Auger Electron Spectroscopy (AES) analyses confirmed elevated concentrations of oxygen, carbon, iron, and transition metals such as Ti, Pt, and S at these locations. These impurities were directly correlated with hotspot formation, highlighting the non-uniform elemental composition in cells.

Skomedal et al. [57] conducted a large-scale case study combining aerial IRTG with production data analysis to investigate thermal anomalies in utility-scale PV plants. Their analysis, based on over 150 strings per site, revealed that the number of module substrings with thermal anomalies is the most critical factor affecting string performance, while the thermal category or hotspot temperature are not. Interestingly, uniformly hot cells (commonly classified as category A anomalies, potentially representative of partial shadings) are generally less detrimental than others, with power losses that could be up to 30% lower than for the case of partial cell heating (type B), hotspots (type C), active bypass diodes (type D), or short-circuited substrings (type E).

Table 2. Thermal images of the bifacial PV panel at different times and camera angles, showing temperature variations under varying irradiance. Measurements were taken at a 6 m distance using a FLIR camera.

Time	**Irradiance**	**Camera Angle**		
		−35°	**0°**	**35°**
09:45	850 W/m^2	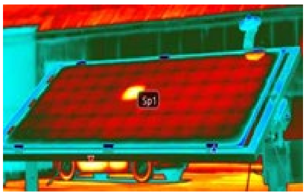	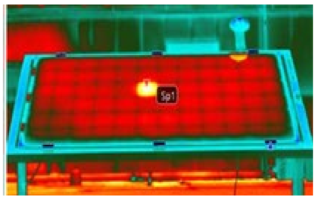	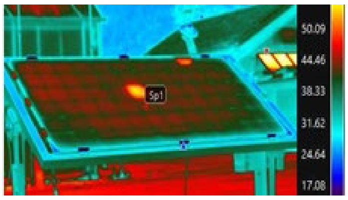
12:50	1005 W/m^2	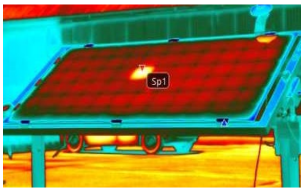	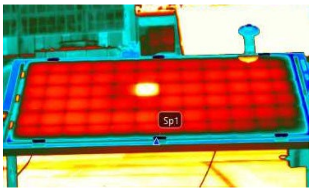	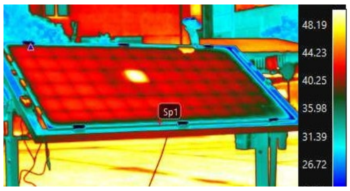
15:20	950 W/m^2	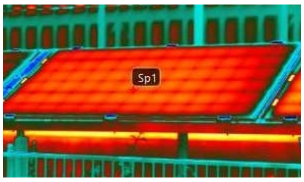	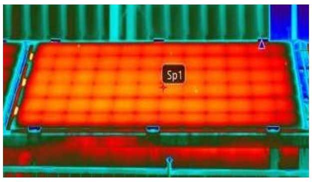	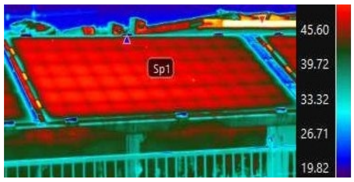

Table 3. Typical hotspot patterns, fault causes, and their impact on module performance identified via infrared thermography.

Pattern	**Fault Reason**	**Description**	**Performance**
	Module is open-circuited—not connected to the system	One module warmer than others	Module normally fully functional
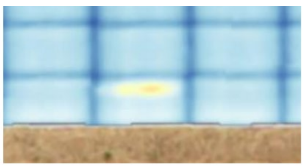	Short-circuited (SC) or open sub-string -Bypass diode SC -Internal SC	One row (substring) is warmer than other rows in the module	Sub-strings power lost, reduction in Voc
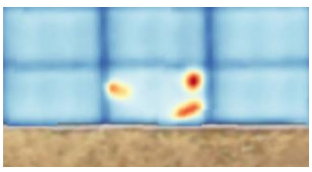	Whole module is short-circuited -All bypass diodes SC -Wrong connection	Single cells are warmer, no pattern (patchwork pattern) is recognized	Check wiring

Table 3. *Cont.*

Pattern	Fault Reason	Description	Performance
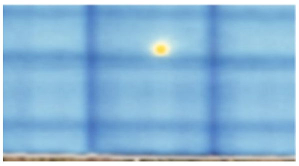	Shadowing effects -Defect cell -Delaminated cell	One cell clearly warmer than the others	Visual inspection needed, cleaning (cell mismatch) or shunted cell
	Artifact -Partly shadowed, e.g., bird dropping lightning protection rod	Pointed heating	Crack detection after detailed visual inspection of the cell possible

3.6. Soiling and Environmental Deposits

Unlike electrically active faults such as hotspots, soiling primarily affects the optical input of photovoltaic modules. However, spatially non-uniform deposits may produce localized temperature differences observable in infrared thermography, which can lead to misinterpretation of thermographic data if not properly identified. Soiling refers to the accumulation of dust, dirt, bird droppings, and other airborne particles on the surface of PV modules, which obstruct sunlight and reduce energy output. This phenomenon is especially critical in arid and semi-arid regions where rainfall is infrequent, and airborne particulates are abundant. Even light soiling can cause measurable power losses, while heavier deposits may lead to hotspot formation and long-term degradation. As a result, monitoring and mitigating soiling effects are essential for maintaining optimal PV system performance. A recent study by Winkel et al. proposes an additional approach to strengthen soiling assessment during PV monitoring. The authors highlight that infrared thermography (IRTG), widely used in drone inspections, can show localized temperature increases that are not necessarily caused by electrical defects but may also originate from spatially inhomogeneous soiling. To reduce the risk of misclassification, they introduce an electrothermal modeling framework that converts spatially resolved soiling information (obtainable from standard RGB aerial images) into predicted temperature maps. By comparing these modeled temperature patterns with measured IRTG images under the same weather conditions, operators can better interpret whether observed temperature non-uniformities are consistent with soiling effects or indicate a more critical module issue, supporting more targeted maintenance actions [46]. In continuation of soiling-related studies, Qasem et al. [83] investigated the impact of dust accumulation on photovoltaic (PV) modules by analyzing spectral transmittance across different tilt angles and dust concentrations. Their findings revealed that dust significantly reduces transmittance, especially at shorter wavelengths (<570 nm), affecting PV performance depending on the cell technology. Amorphous silicon cells, due to their wide bandgap, exhibited the highest photocurrent loss up to 33% at a dust density of 8.5 mg/cm^2 followed by crystalline silicon and copper–indium–gallium selenide (CIGS) modules with 28.6% and 28.5% losses, respectively. The study also highlighted that tilt angle influences non-uniform dust distribution, with the 30° tilt showing the greatest non-uniformity in spectral transmittance. These results underscore the importance of considering spectral and positional soiling effects in performance modeling and maintenance strategies for PV systems, particularly in dust-prone environments like Kuwait. Figure 16, illustrates non-uniform dust accumulation across PV modules in Kuwait, highlighting the impact of harsh environments on soiling patterns.

Figure 16. Accumulated dust on different PV modules installed in Kuwait, showing varying soiling patterns and intensities.

4. Methods of Fault Detection

Reliable fault detection strategies are essential for minimizing energy losses and preventing accelerated degradation in large-scale PV installations. As PV installations continue to scale globally, timely identification of faults—ranging from microcracks to hotspots—and PID become essential for preventing energy losses and mitigating long-term degradation. Various detection methods have been developed, each with specific advantages, sensitivities, and application contexts. These include visual inspections, electrical testing, and advanced imaging techniques such as IRTG, EL (electroluminescence), PL (photoluminescence), and ultraviolet fluorescence (UVF). The following subsections provide a thematic analysis of the most widely used fault detection approaches, highlighting their principles, strengths, and limitations in real-world PV diagnostics.

4.1. Visual Inspection

Visual inspection is commonly used as a preliminary diagnostic method to identify macroscopic defects such as cracks, discoloration, and delamination before applying more advanced diagnostic techniques. While limited to surface-level faults, it helps flag modules needing further analysis. Djordjevic et al. [45] analyzed numerous rooftop PV installations across Australia and highlighted common visually detectable issues, including microcracks, snail trails, and discoloration. Their findings showed that while some defects may appear visually concerning, many have a limited impact on module output and can be managed without significant loss of system reliability. As also highlighted by Mik et al. [84], the effect of snail tracks on module performance is expected to be marginal, but decoupling its influence from the other failures is challenging: in fact, for example, the authors noted that visually detected snail tracks are related to microcracks in 96% of the occurrences. However, in cases involving severe physical impacts due to weather, mishandling, or vandalism, visual inspection successfully revealed extensive glass breakage and structural faults that correlate with measurable power loss. The study reinforces visual inspection's utility as a cost-effective, first-line method for identifying modules that may require closer evaluation or replacement: an indispensable first-line diagnostic tool, visual inspection identifies modules needing further investigation, enabling targeted deployment of resource-intensive techniques like IR thermography or EL imaging. This hierarchical approach, using visual inspection as a preliminary filter, optimizes maintenance workflows by concentrating advanced diagnostics on modules with confirmed physical anomalies, reducing costs and minimizing downtime.

4.2. Electrical Pulsed Infrared Thermography

Electrical Pulsed Infrared Thermography (EPIT) is a defect detection technique that leverages controlled electrical excitation and thermal imaging to localize structural and electrical anomalies in PV cells. As illustrated in Figure 17, a programmable DC power supply applies a forward bias to the PV panel, inducing diffusion and recombination currents. In the presence of defects, such as scratches, hidden cracks, or gate breaks, localized recombination at defect sites leads to disproportionate heat generation, which alters the surface temperature distribution of the cell. An infrared (IR) camera, positioned to capture thermal emissions, records these variations and transmits the data to a computer via a data acquisition (DAQ) card. This results in a sequence of thermographic images that visually map the cell's surface temperature. Post-processing using supervised learning algorithms such as Linear Discriminant Analysis (LDA) and Quadratic Discriminant Analysis (QDA) enhances the visibility of defect features by maximizing spectral contrast between defective and non-defective regions. Experimental results confirm EPIT's effectiveness in identifying various PV cell faults with high signal-to-noise ratios, particularly when using QDA for defect classification.

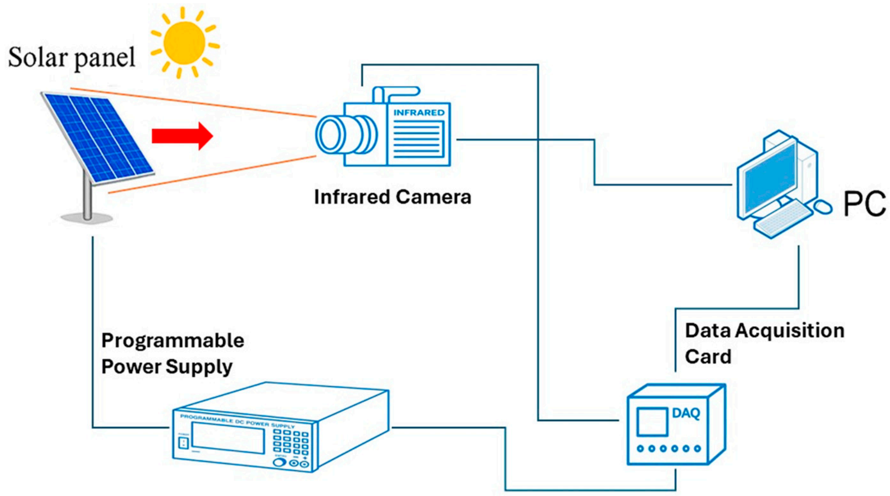

Figure 17. Schematic of the Electrical Pulsed Infrared Thermography (EPIT) setup for PV fault detection. A programmable power supply biases the solar panel, inducing localized heating at defect sites, which is captured by an infrared camera and processed through a data acquisition system and PC for thermal analysis.

EPIT was experimentally implemented by Bu et al. [85] to detect and classify multiple PV cell defects, including broken gates, hidden cracks, scratches, and hotspots. In their study, two polysilicon solar cells were tested using a programmable power supply providing pulsed forward bias excitation, while thermal images were recorded by a FLIR SC655 infrared camera at a sampling rate of 20 Hz. The acquired thermography sequences were processed using Linear Discriminant Analysis (LDA) and Quadratic Discriminant Analysis (QDA) to enhance defect visibility. Their results demonstrated that the QDA algorithm outperformed LDA and Principal Component Analysis (PCA), yielding higher signal-to-noise ratios (SNRs) and clearer identification of hidden cracks and hotspot regions. Optimal bias voltages between 1 V and 1.5 V enabled effective defect recognition with temperature differentials of 11.5–14.9 °C for scratched cells and 6.4–8.4 °C for hotspots. EPIT, when integrated within supervised learning-based diagnostic frameworks, constitutes an effective approach for early-stage fault detection in PV cells, enabling the identification of subtle defect signatures and supporting proactive maintenance strategies.

https://doi.org/10.3390/en19061570

4.3. Electroluminescence (EL) Method

The EL technique is a well-established visual testing method used in photovoltaic diagnostics and is often employed as a complementary technique to infrared thermography (IRTG) for detecting defects that may not produce observable thermal signatures [86–88]. Recent studies integrating EL imaging with machine learning frameworks have demonstrated fault classification accuracies exceeding 95–99%, depending on dataset conditions and noise levels. Moreover, advanced feature-extraction approaches applied to PV fault diagnostics have reported overall detection accuracies above 97%, confirming the capability of image-based and data-driven techniques to reliably distinguish between normal and faulty states [88]. Unlike infrared thermography, which primarily detects thermally active defects, electroluminescence (EL) imaging is particularly effective for identifying electrically inactive defects such as microcracks or inactive regions that may not generate detectable thermal signatures [89–91]. In large-scale experimental validation involving 126 multi-defect PV module images, CNN-based EL image analysis achieved defect classification accuracies exceeding 95% across all defect categories, with reported averages of 98.42% for glass breakage, 98.59% for encapsulation delamination, and 95.03% for snail trails, confirming the robustness of image-driven defect recognition frameworks [89]. Comparative evaluation further demonstrated that such deep-learning-based approaches significantly outperform conventional pattern-recognition methods (typically 55–80% accuracy) and pretrained generic CNN architectures (≈51–75%), highlighting the importance of domain-specific feature extraction in PV defect diagnostics [89]. By applying a forward DC current, radiative recombination is stimulated in the solar cells, emitting infrared radiation. This emission is captured using a CCD (charged-coupled device) camera in a dark environment to produce high-resolution EL images that reveal internal structural issues not visible to the naked eye.

Figure 18 illustrates two common crack modes detectable through EL The left image corresponds to "Crack Modus A," where a visible crack exists, but it does not interrupt current flow across the cell, indicating no added resistance. In contrast, the right image represents "Crack Modus B+(A)," where the crack begins to affect current flow toward the interconnect ribbon, though the cell remains electrically connected. These subtle internal changes, distinguishable through EL imaging, enable early and accurate fault classification. The technique is highly sensitive, making it an invaluable tool in quality control and post-installation diagnostics.

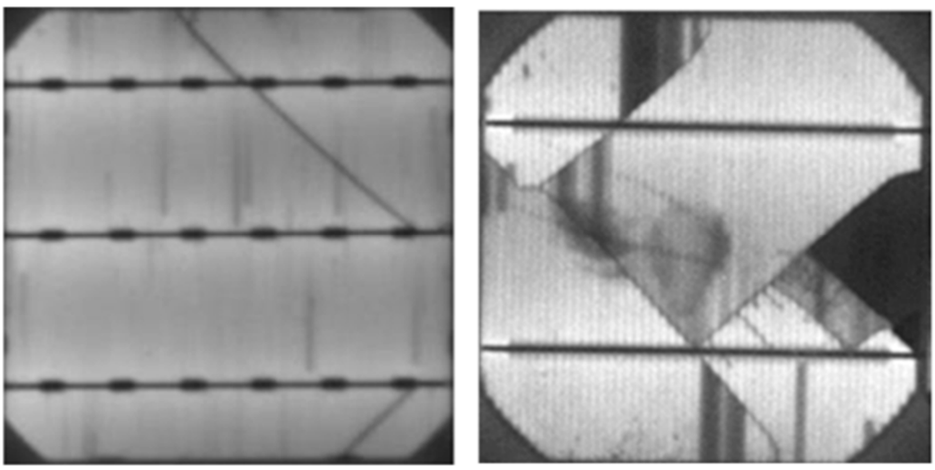

Figure 18. EL images of solar cells showing: (**left**) crack without impact on current flow (Modus A); and (**right**) crack partially affecting current flow to the interconnect (Modus B+(A)) [92].

Akram et al. [93] proposed a lightweight deep learning-based approach for automatic defect detection in photovoltaic cells using EL images. Although EL imaging differs from IRTG in physical principle, capturing radiative recombination patterns rather than surface temperature distributions, the study is relevant in the context of AI-driven diagnostic frameworks for PV systems. The authors developed a CNN architecture achieving 93.02% classification accuracy on a publicly available EL dataset, with real-time inference capability (8.07 ms per image on a standard CPU). While the input modality differs from thermographic data, the methodological framework comprising data augmentation, L2 regularization, batch normalization, and dropout demonstrates transferable strategies for improving robustness and generalization in image-based PV defect detection. In thermographic applications, similar CNN-based architectures are increasingly employed to classify hotspot patterns, bypass diode failures, and interconnect degradation under varying environmental conditions. Therefore, this study is discussed as a complementary AI methodology rather than a thermography-specific application, illustrating the broader integration of deep learning techniques in PV diagnostic imaging.

4.4. Infrared Thermography (IRTG)

IRTG is a widely adopted non-contact diagnostic technique used for inspecting PV systems under real operating conditions [25,94–96], with active methods such as vibrothermography achieving complete inspection cycles in as little as 2.4 s per wafer [10]. It detects temperature anomalies on the surface of modules, which often indicate hidden faults like hotspots, soldering issues, or cell fractures. This method enables rapid and safe assessment across large installations without interrupting energy production.

In a study by Buerhop et al. [97], fifteen PV plants were examined using IR imaging, EL analysis, and power measurements across 260 dismantled modules. The study confirmed IRTG's effectiveness in identifying failures such as bypassed substrings, fractured cells, and short-circuited areas. These faults led to critical temperature differences, i.e., up to 45 °C, and directly correlated with significant drops in power output. Notably, all modules with elevated temperature zones were found to be defective. Figure 19 illustrates a practical IR overview of a rooftop PV plant under real conditions, where five modules (e.g., 1.12, 2.11, 2.15, 4.14, 6.15) show abnormal heating patterns, clearly visible as red patches, demonstrating IRTG's capability to quickly flag underperforming units.

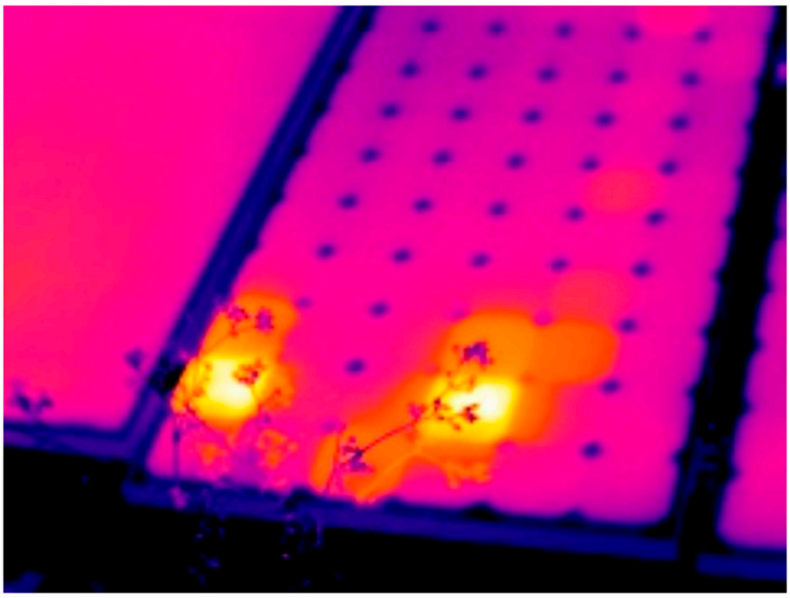

Figure 19. Typical ground-level infrared thermographic image of a ground-mounted PV module under normal operation, highlighting two major irregular cell heating [98].

4.5. Aerial Infrared Thermography

Aerial Infrared Thermography (aIRTG) is a fast, non-invasive, and cost-effective technique increasingly used for monitoring utility-scale PV systems. By mounting infrared cameras on drones, aIRTG enables efficient fault detection across large areas without interrupting system operation [99,100], reducing inspection time by a factor of 10–15 compared to conventional ground-based methods [10]. This method is particularly advantageous for early-stage defect identification and preventative maintenance in remote or large solar installations, where manual inspections are labor-intensive or impractical. Studies such as those by Bizzarri et al. [101] and Cioaca et al. [102] demonstrate that drone-based IR inspection significantly reduces maintenance costs and diagnosis time while improving diagnostic accuracy, especially when thermal and RGB imaging are combined. Tsanakas and Botsaris [103] further reinforced the method's diagnostic power by applying histogram and line profile analysis to thermal images, effectively localizing and quantifying hotspots and module degradation. In a more recent campaign, Vidal de Oliveira et al. [104] examined four utility-scale PV plants in Brazil, revealing that the most common faults were disconnected substrings and strings, with disconnected strings contributing most to power losses. Their results showed that RGB-assisted inspection helped distinguish actual faults from soiling or vegetation shading, enhancing diagnostic reliability. Additionally, post-flight image analysis proved more time-efficient than real-time evaluation, optimizing labor use. Recent integration of machine learning algorithms has further enhanced diagnostic capabilities: convolutional neural networks achieve >99% accuracy in hotspot detection with localization errors as low as 0.86 m, while support vector machine models correctly classify over 96% of thermal anomalies [10]. Overall, aIRTG has proven to be a reliable tool for maximizing uptime, reducing maintenance costs, and supporting condition-based monitoring in modern PV asset management.

An illustrative case is shown in Figure 20, where a false hotspot was detected on a module due to bird droppings. The infrared image on the left highlights a localized heat anomaly, which initially appears to indicate a fault. However, the corresponding RGB image on the right confirms the actual cause, i.e., external soiling rather than an electrical defect. This example underscores the importance of integrating thermal and visual data during inspections to accurately interpret results and avoid misdiagnosis.

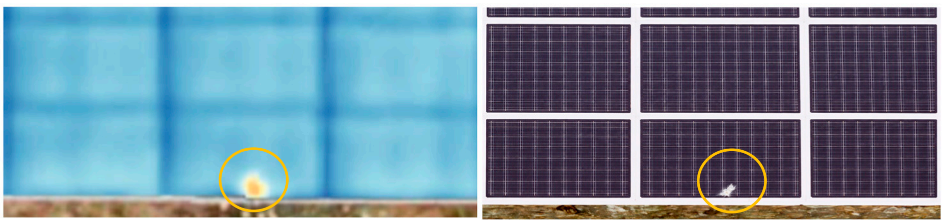

Figure 20. Aerial infrared and RGB images of a PV plant showing a false hotspot caused by bird droppings. The IR image (**left**) indicates a temperature anomaly, while the RGB image (**right**) clarifies the non-electrical nature of the defect.

In this regard, the problem of detection accuracy has also been tackled in [32], in which the mean thermal intensity and standard deviation were used as key metrics; in order to move beyond qualitative interpretation of thermal imaging results, the authors established establishing statistical thresholds at the array level rather than applying global rules. Quantitative temperature thresholds and standardized classification criteria for PV defect diagnosis are proposed by [105]. The authors propose a "Thermal Pixel Counting" algorithm that establishes specific temperature differential indices (i.e., ΔT = 15 °C and 20 °C above minimum panel temperature), so that surface temperatures exceeding these values indicate power loss and safety concerns classified under specific classes. In general, the absence of standardized ΔT thresholds for PV thermal fault diagnosis is widely acknowledged in the literature; for example, ref. [106] explicitly notes this lack of consensus while proposing a categorization framework based on IEC TS 62446-3. The authors classify defects into single hotspots, multiple hotspots, uniform substrings, uniform modules, and uniform strings, further subcategorizing hotspots by severity using temperature differentials: 2–7 K for mild, 7–10 K for intermediate, and >10 K for severe anomalies. Infrared-based fault classification in photovoltaic systems still lacks universally standardized diagnostic criteria. Commonly adopted ΔT thresholds (e.g., 5 K, 10 K, 20 K) are largely empirical and derived from specific case studies, which limits their transferability across different environmental and operational conditions. Moreover, reported failure rates are not consistently disclosed in the literature, and when available, they are often based on heterogeneous datasets and methodologies, making cross-study comparisons and the definition of universally applicable quantitative benchmarks inherently challenging.

4.6. Unmanned Aerial Vehicles (UAVs)

UAVs have revolutionized PV inspection practices, offering fast, efficient, and cost-effective monitoring, especially for large-scale photovoltaic plants. UAVs equipped with infrared and visual cameras can detect a wide range of faults, including hotspots, disconnected substrings, shading, and physical damage, without interrupting system operation. Bellezza Quater et al. [107] demonstrated that UAV-based thermal inspections significantly outperform traditional methods in terms of speed and cost, successfully detecting various PV module failures across a 200 kW PV system in northern Italy. Their trials confirmed the reliability of thermal cameras mounted on light UAVs to rapidly assess system performance in real time. Similarly, Aghaei et al. [108] introduced a smart UAV system capable of real-time infrared thermographic inspection, automatically identifying degraded modules for further evaluation. The system proved adaptable to different weather conditions and PV configurations, using threshold-based alerts to flag modules with more than 5% degradation. Further advancements in automated image analysis and historical data comparison are expected to refine these systems for long-term operation and maintenance strategies. Coello et al. [109] emphasized the practical benefits of UAV deployment, noting that aerial inspections can reduce thermographic assessment times by up to 85%, making them ideal for inspecting extensive or hard to access PV installations.

Grimaccia et al. [110] further explored the potential of UAVs in enhancing the operation and maintenance (O&M) strategies of photovoltaic energy systems through experimental validation on a real 3 MW PV plant comprising approximately 12,600 polycrystalline modules over a 350×120 m^2 area. Their study focused on using lightweight UAVs equipped with GPS and thermal imaging systems to perform coordinated inspections. A key innovation in their approach was the implementation of cooperative route mapping: comparison between horizontal and vertical flight paths demonstrated a reduction in total traveled distance from 2.71 km to 2.02 km, corresponding to approximately 25% shorter inspection distance, thereby improving time and energy efficiency of monitoring operations. From an economic perspective, the authors estimated that for a 1 MW PV plant (with an annual O&M cost of roughly \$50 kW^{-1}, i.e., ≈\$50,000 per year), UAV-based inspections would increase annual maintenance costs by only 6–10%, while enabling earlier detection of underperforming modules and reducing long-term performance degradation risks. The UAV platform used (2.8 kg weight, 0–20 kts cruise speed, 0.25–0.4 h endurance) demonstrated practical field applicability under real operating conditions.

These results quantitatively confirm that UAV-assisted thermography can significantly improve inspection efficiency, reduce travel distance and operational time, and provide economically scalable monitoring for medium to large PV plants.

As highlighted in the IPCC's (Intergovernmental Panel on Climate Change) Fifth Assessment Report (AR5), addressing climate change requires reliable, science-based strategies for monitoring and managing energy systems, particularly under increasing risks of extreme weather and long-term environmental shifts. In this context, UAVs offer a practical, efficient tool for supporting climate adaptation in the renewable energy sector. Their ability to rapidly inspect large-scale PV systems aligns with the AR5's emphasis on improving resilience and operational efficiency through enhanced observational capabilities. By enabling early detection of faults and degradation in PV modules, UAV-based monitoring contributes to more sustainable energy production, helping mitigate energy losses and ensure system reliability in the face of changing climate conditions [111].

Elmokadem and Savkin [112] conducted a comprehensive survey of recent developments in unmanned aerial vehicles UAVs, with a particular focus on autonomous navigation systems. Their study emphasizes that achieving fully autonomous UAV operations is increasingly feasible due to rapid advances in motion planning, control strategies, perception, and localization. Quantitatively, standard GPS-based navigation typically provides positioning accuracy on the order of 2–5 m, while integration with RTK-GPS systems enables centimeter-level precision, significantly improving flight path reliability for infrastructure inspection tasks. Furthermore, modern UAV platforms commonly achieve 20–60 min of flight endurance, allowing substantial area coverage per mission, while real-time obstacle detection systems operate at update rates exceeding 10 Hz, supporting safe navigation in complex environments. A significant contribution of their work is the exploration of advanced 3D collision free navigation algorithms, which reduce path redundancy and improve trajectory efficiency compared to basic waypoint navigation. The authors also highlight that coordinated multi-UAV systems can further decrease mission duration relative to single UAV deployments, enhancing inspection scalability [112]. While primarily theoretical, the review identifies remaining challenges such as robust real-time decision-making and distributed coordination under uncertain environmental conditions. For renewable energy monitoring applications, these quantified improvements in navigation precision, endurance, and coordination directly translate into reduced inspection time, improved coverage reliability, and more consistent thermal data acquisition across large-scale PV installations.

UAVs can be broadly classified based on their control configurations, which determine their flight mechanics and application suitability. The most common types include multirotor UAVs, such as hexacopters, known for their hovering capability and maneuverability, and fixed wing UAVs, which are more efficient for covering large areas at higher speeds. Figure 21 illustrates these two configurations: the left image shows a multirotor hexacopter, suitable for precise, localized inspections, while the right image shows a fixed wing UAV, better suited for long range surveillance tasks such as large-scale PV plant monitoring. Each category offers unique advantages depending on the inspection requirements and environmental conditions.

Figure 21. UAV types used in PV inspection: (**left**) multirotor hexacopter ideal for detailed, localized monitoring; (**right**) fixed wing UAV suitable for long range, large area surveillance [112].

Evstatiev et al. [113] experimentally evaluated the accuracy and uncertainty of thermographic inspections in a 12.6 kWp PV plant (36 modules, 350 W each) by comparing contact DS18B20 sensor readings with infrared measurements obtained from close (2 m) and remote distances (15–26.9 m). Under hotspot conditions, the absolute temperature difference between close range and remote IR measurements reached up to 34.1 °C, with relative deviations exceeding 30–50%, while discrepancies between remote IR and contact sensors generally remained below 10 °C (~16%). Intra-cell temperature gradients were found to exceed 40 °C, and hotspot to neighboring cell differences surpassed 50 °C, demonstrating significant spatial non-uniformity. Importantly, no hotspot formation was observed when less than 6% of the cell surface was covered, indicating a practical detection threshold for IR inspections. These results quantitatively confirm that UAV-based thermography is strongly influenced by distance, resolution, and viewing geometry, and that uncertainty in peak temperature estimation must be considered when interpreting large-scale PV inspections. Overall, UAV-based monitoring represents a transformative advancement in PV system inspection, combining flexibility, precision, and automation in one platform. Beyond their ability to detect thermal anomalies and structural defects, UAVs offer scalable, non-intrusive, and rapid data collection for both small-scale and utility-scale installations [114]. Their deployment minimizes inspection time, reduces operational downtime, and enhances worker safety by eliminating the need for manual access to elevated or remote structures. With continuous improvements in imaging technology, autonomous navigation, and onboard data processing, UAVs are becoming an indispensable tool for predictive maintenance and real-time performance analysis of PV systems. This integrated approach ensures sustained energy yield, optimizes maintenance scheduling, and supports the long-term reliability of solar power infrastructure. Table 4 summarizes the reviewed fault detection methods, including their principles, advantages, and limitations. Visual inspection remains useful for rapid, low-cost checks, while EL and IRTG offer higher diagnostic accuracy. UAV-based inspections improve coverage and safety for large-scale plants, and soiling analysis addresses environmental performance losses. Together, these approaches provide a complementary framework for reliable and proactive PV monitoring.

Table 4. Comparative overview of key PV fault detection methods, highlighting their principles, advantages, limitations, and application characteristics.

Methods Type	Principle/Technique	Advantages	Limitations/ Challenges	Complexity	Accuracy/ Sensitivity	Ref.
Visual Inspection	Manual or drone-assisted visual assessment of surface defects (cracks, delamination, discoloration, snail trails)	Low-cost, simple, immediate defect detection; no equipment needed	Limited to visible surface faults; subjective interpretation; cannot detect internal defects	Low	Low–Moderate	[45]
Electrical Pulsed Infrared Thermography (EPIT)	Pulsed electrical excitation and thermal imaging to reveal heat signatures from electrical defects	High defect localization accuracy; detects hidden cracks and hotspots; non-destructive	Requires controlled bias and calibration; not suitable for large-scale field inspections	Moderate	High	[85]
Electroluminescence (EL)	Forward bias induces radiative recombination captured by CCD cameras in dark conditions	High spatial resolution; detects microcracks, inactive areas; quantitative image analysis possible	Requires darkness; not suitable for full-scale plants during daytime; needs DC excitation	High	Very High	[93]
Infrared Thermography (IRTG)	Measures emitted thermal radiation to identify abnormal temperature regions	Non-contact, fast, reliable under operation; detects hotspots, solder faults, PID	Sensitive to environmental conditions (irradiance, wind); cannot distinguish soiling vs. defects alone	Moderate	High	[97]

Table 4. *Cont.*

Methods Type	Principle/Technique	Advantages	Limitations/ Challenges	Complexity	Accuracy/ Sensitivity	Ref.
Aerial Infrared Thermography (aIRTG)	Drone mounted IR and RGB imaging for large-scale inspection	Rapid coverage, no downtime, detects thermal anomalies and soiling; cost-effective	Requires skilled operation; influenced by altitude, wind, and lighting; data processing intensive	Moderate	High	[101,104]
Unmanned Aerial Vehicles (UAVs)	UAVs equipped with IR, RGB, and multispectral sensors for automated fault detection	High-speed, scalable inspection; enhances worker safety; adaptable for autonomous operation	Accuracy depends on flight altitude, camera calibration, and environmental factors	Moderate–High	High	[107,110,113]
Soiling Analysis	Measurement of dust accumulation and its spectral impact on light transmittance	Identifies energy loss causes; essential for cleaning and maintenance scheduling	Region-specific; difficult to automate; requires long term monitoring	Low–Moderate	Moderate	[83]

4.7. Summary of Section 4: Methods of Fault Detection

This section provides a comprehensive review of contemporary fault detection methods for PV systems, each addressing different diagnostic needs, operational contexts, and fault types. Beginning with visual inspection, this traditional approach remains essential for identifying macroscopic defects such as discoloration, delamination, and mechanical damage. While limited to surface-level anomalies, studies confirm its cost-effectiveness and utility in flagging modules for further analysis. Electrical Pulsed Infrared Thermography (EPIT) offered a more advanced approach, using controlled forward-bias excitation and infrared imaging to localize internal electrical faults like hidden cracks or broken gates. When combined with supervised learning techniques such as Quadratic Discriminant Analysis (QDA), EPIT has demonstrated high signal-to-noise ratios and robust defect classification, making it particularly suitable for laboratory-scale diagnostics and early-stage quality control.

EL imaging emerged as a high-resolution, non-invasive technique capable of detecting microcracks, inactive regions, and other latent defects. Its sensitivity to minute changes in current pathways enables early identification of performance-degrading issues. Notably, the integration of lightweight deep learning models has shown great promise in automating defect detection with high accuracy and real-time inference capability, pushing EL further toward field-deployable solutions.

IRTG, a broadly adopted non-contact technique, has proven invaluable for large-scale inspections under real-world conditions. IRTG reliably detects hotspots, soldering defects, and cell fractures by identifying thermal anomalies. Studies across dismantled PV plants confirmed a strong correlation between elevated temperature zones and reduced power output, highlighting IRTG's diagnostic power. However, IRTG's accuracy may be limited by environmental factors such as wind and irradiance, necessitating careful calibration and contextual interpretation.

Building upon IRTG, Aerial Infrared Thermography (aIRTG) leveraged UAV-mounted thermal and RGB cameras to inspect utility-scale PV systems efficiently. Campaigns in Brazil revealed that aIRTG could identify disconnected substrings, shading from vegetation, and other critical faults that impact system performance. Post-flight image analysis proved more efficient than real-time assessments, and the integration of RGB imaging improved fault classification by differentiating between true hotspots and external soiling.

UAVs, as a general inspection platform, have been reviewed extensively. Various UAV types—such as multirotor and fixed-wing models—offer distinct advantages depending on inspection scope and terrain. Case studies in Italy and Bulgaria demonstrated that UAVs, equipped with thermal and visual cameras, automatically detect degraded modules, and adapt to varying environmental conditions. Importantly, experiments showed significant discrepancies in temperature readings based on measurement angle and sensor proximity, reinforcing the need for multi-sensor integration. Recent developments in autonomous navigation and cooperative UAV routing also promise to enhance scalability and reduce human intervention in PV monitoring. Moreover, UAVs align with global climate resilience goals, offering tools to support rapid, data-driven decisions in renewable energy infrastructure management. The soiling subsection addressed one of the most pervasive environmental challenges to PV performance. Dust accumulation, as demonstrated in studies from Kuwait, can significantly impact transmittance, especially in the UV and visible spectra (<570 nm), leading to up to 33% power losses in wide bandgap technologies such as amorphous silicon. The tilt angle and dust distribution also affect optical uniformity, emphasizing the need for context-specific soiling models. Observational data confirmed that minor soiling below 6% surface coverage might remain undetectable by thermal imaging alone, supporting the recommendation to use visual cameras in conjunction with IR systems. Figure 20 vividly illustrates non-uniform soiling patterns across modules, highlighting the real-world relevance of such environmental degradation.

Collectively, this section highlights that an integrated approach combining surface-level observations, thermal analysis, luminescence imaging, and airborne surveillance offers the most robust framework for fault detection, performance optimization, and long-term reliability in photovoltaic systems. As system sizes grow and operational complexity increases, the adoption of automated, multi-modal inspection strategies will be pivotal in supporting efficient maintenance, reducing energy losses, and achieving sustainable energy goals.

5. Inspection Algorithms and Challenges

With the increasing adoption of infrared thermography, electroluminescence imaging, and UAV-assisted inspections for PV systems, the role of advanced computational algorithms has become essential. Central to these developments is the application of image processing techniques [115], which play a pivotal role in enhancing, analyzing, and interpreting large volumes of visual and thermal data collected from PV modules. These algorithms are used to detect, classify, and localize faults such as hotspots, cracks, delamination, and shading with high precision. Traditional manual inspection is no longer scalable or efficient for large-scale solar installations. Instead, modern inspection pipelines increasingly rely on automated image processing applications, computer vision methods, and ML models, including deep learning architectures, to streamline data analysis and decision-making. These tools not only enhance detection accuracy but also minimize human error, enable real-time diagnostics, and support predictive maintenance strategies. Despite its effectiveness in fault localization, classical thermographic inspection is inherently qualitative. Thermal gradients indicate anomalies but cannot alone establish a universally applicable degradation model, due to environmental variability and technology-dependent responses. For this reason, recent research focuses on hybrid and data-driven approaches to improve robustness and reproducibility. Although thermal imaging can reveal abnormal heating patterns, translating these temperature variations into quantitative degradation pathways remains challenging. Similar thermal signatures may arise from different physical mechanisms, and environmental variability further limits reproducibility. Consequently, IRTG should not be considered a standalone quantitative degradation modeling tool.

5.1. Digital Image Processing (DIP)

Digital image processing techniques are widely employed in PV inspections to enhance thermal and visual images and to facilitate the automatic detection of defects such as microcracks, hotspots, and delamination. The main task of image processing techniques is to treat the images by applying appropriate signal and filtering operations to enhance the visibility of fault signatures and remove noise or distortions before analysis [116]. In PV applications, DIP enables the identification of anomalies such as microcracks, hotspots, delamination, or soiling through enhancement, segmentation, and feature extraction steps. These techniques are now widely deployed in automated PV inspections, as they help isolate defective regions and prepare structured data for higher-level classification or diagnostic algorithms. As demonstrated in recent studies, DIP is increasingly integrated as a core module in computer vision pipelines for PV condition monitoring and predictive maintenance [117]. Also, many digital-image processing techniques exploit the electromagnetic spectrum by applying noise filtering, edge detection, and sparsity-based methods to enhance and analyze image content [118].

5.2. Machine Learning (ML) and Hybrid AI-Based Methods

Recent studies increasingly apply ML algorithms to automate the interpretation of thermographic and electroluminescence images in PV diagnostics. In PV inspections, ML algorithms are trained to classify defects such as hotspots, cracks, and delamination by recognizing complex patterns within large image datasets often collected via infrared thermography or electroluminescence imaging. These data-driven models, ranging from traditional classifiers like support vector machines (SVMs) to deep neural networks, significantly enhance fault detection speed and reliability compared to manual or rule-based approaches. Notably, DIP can even be combined with deep learning (DL) models to leverage the strengths of both, applying advanced feature extraction from DIP with the powerful classification capabilities of DL to automate image recognition and defect identification with minimal human intervention, as highlighted in [119]. DL focuses on accurately extracting and classifying complex patterns from data using CNNs as a core architecture for visual tasks in PV fault detection [120]. By continuously learning from new data, ML-based approaches ensure robust performance across varying environmental and operational conditions, making them indispensable in modern PV monitoring and forecast-based maintenance systems. A recent advancement in this direction is presented in [46], where a hybrid AI-based defect detection framework was developed by integrating infrared thermal images with electrical I–V curve characteristics. Unlike single-modality approaches, this method exploits the complementary nature of surface temperature distributions and electrical performance signatures to improve diagnostic robustness. As illustrated in Figure 22, thermal images and I–V curves are processed through convolutional and pooling layers for feature extraction, followed by fully connected layers that fuse multimodal representations to classify operating conditions such as normal behavior, dust accumulation, cracks, partial shading, and short-circuit faults. Using a transfer-learning strategy based on a VGG16 convolutional architecture, the system enables parallel feature learning from both image and electrical inputs, substantially enhancing fault discrimination. Experimental validation on rooftop PV modules demonstrated accuracy and recall exceeding 98%, confirming that multimodal learning can outperform conventional single-input ML pipelines by jointly capturing visible thermal anomalies and latent electrical degradation.

Furthermore, the study highlights the practical advantages of hybrid AI frameworks for real-world PV monitoring, particularly under harsh environmental conditions. By leveraging data augmentation and fine-tuned transfer learning, the proposed model maintained strong generalization despite limited datasets while reducing computational requirements compared to training deep networks from scratch. Importantly, the fusion of thermal imagery with I–V curve analysis enabled more reliable detection of defects that may not be evident from temperature patterns alone, thereby mitigating false negatives. These findings reinforce the growing trend toward integrated, data-driven inspection pipelines, where ML models combine imaging and performance metrics to support proactive maintenance, scalable deployment, and higher-confidence decision-making in large-scale photovoltaic systems [46].

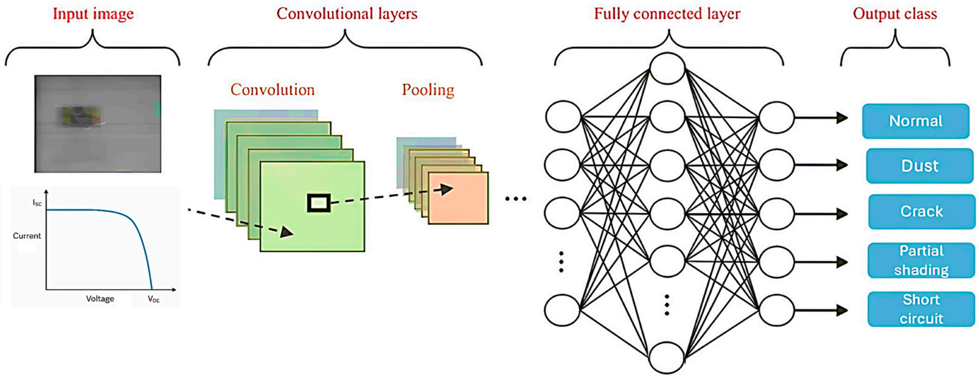

Figure 22. Schematic of the hybrid CNN-based defect detection framework integrating infrared thermal images and I–V curve inputs. Convolutional and pooling layers extract multimodal features, which are fused through fully connected layers to classify PV operating states such as normal operation, dust, cracks, partial shading, and short-circuit faults [46].

5.3. Convolutional Neural Networks (CNNs)

CNNs [121] are among the most widely adopted deep learning models for fault detection and image classification [122–124] in PV systems. As a class of deep neural networks specifically designed for image analysis, CNNs excel at extracting spatial features from visual, thermal, or EL images of PV modules. Their layered architecture enables automatic learning of hierarchical features, making them highly effective for identifying microcracks, delamination, hotspots, and other defects. CNNs eliminate the need for manual feature engineering and demonstrate strong robustness to image noise, variable lighting, and scale distortions, which are common in real-world inspection scenarios. By leveraging CNNs within automated inspection systems, especially when integrated with UAVs or drone-acquired imagery, operators can significantly enhance the scalability, accuracy, and speed of PV system diagnostics across both rooftop and utility-scale installations [125].

5.4. Critical Perspective on Current Thermographic Approaches in PV Diagnostics

A critical review of the existing literature reveals several persistent challenges that remain insufficiently addressed. Despite the widespread adoption of infrared thermography as a non-invasive diagnostic tool for PV systems, important cross-cutting gaps continue to limit its full standardization and practical optimization.

Although IEC TS 62446-3 provides structured guidance for outdoor infrared inspections of PV modules and systems under natural sunlight, it remains a Technical Specification intended to standardize inspection procedures rather than define quantitative acceptance criteria [126]. Unlike IEC 61215, which establishes pass/fail requirements based on electrical performance metrics, infrared thermography does not directly quantify the electrical impact of detected thermal anomalies on I-V characteristics. Consequently, temperature deviations observed through IRTG cannot be universally translated into performance-loss thresholds or failure criteria. Field studies and practical inspection campaigns further show considerable variability in how these recommendations are implemented, including differences in irradiance thresholds [30], wind influence, viewing-angle effects on emissivity and reflectance, and the radiometric calibration and measurement uncertainty of infrared cameras [127]. These intrinsic limitations of IRTG, particularly its indirect relationship with electrical degradation and its sensitivity to environmental and instrumentation factors, preclude the formulation of standardized pass/fail criteria within IEC TS 62446-3 and complicate the definition of universally applicable temperature-based severity classifications. Therefore, IRTG should be regarded primarily as a qualitative or semi-quantitative screening tool rather than a definitive compliance-testing method. A second challenge concerns the limited correlation between the temperature anomaly pattern and quantitative performance degradation. Although several works report empirical relationships between hotspot temperature and string-level energy losses, a generalizable model that accounts for module architecture, bypass diode behavior, shading dynamics, and aging mechanisms is still missing. Without such models, thermography remains predominantly qualitative [42]. Recent works, such as [11], demonstrate that the correlation between hotspot patterns and performance degradation over time is weak, and only the number of faulted modules (with thermal anomalies) on the same PV string has a measurable impact on performance decay.

There is a clear research gap at the intersection of thermography and data-driven methods. Even though deep learning models for detecting PV module defects have considerably improved, most of them are trained on carefully selected datasets that do not represent the variability seen in real PV plants [128], and the dataset used in [129]. Also, a strong domain-shift problem can be recognized: models trained in the lab or on ground-based thermal images usually are less effective on UAV-acquired images from real PV plants. Additionally, the lack of public thermal datasets with good annotations complicates reproducing results or comparing models. It should also be emphasized that most datasets focus on monofacial modules, while bifacial modules add extra challenges, like rear-side irradiance, reflections, and different thermal patterns, which current models are usually not trained for [130].

The growing adoption of UAV-based thermography introduces additional measurement challenges. Flight altitude, camera pitch and roll [131], platform vibration [132], and variable atmospheric transmissivity all contribute to uncertainty [106], yet these sources of error are rarely quantified in PV inspection studies. Many publications employ a single flight configuration without assessing how sensitive thermal results are to different flight parameters, which restricts the applicability of their findings across different plants and conditions. Multi-modal diagnostic strategies that integrate thermography with EL, PL, IV curve analysis, or SCADA data remain largely underexploited. Several fault types, such as early-stage PID, microcracks, or metallization corrosion, often produce weak or undetectable thermal signatures, making thermography alone insufficient for reliable detection. The lack of systematic frameworks to fuse electrical and thermal information constrains the overall diagnostic completeness of field inspections, limiting the ability to accurately identify and quantify module or string-level faults.

Addressing these gaps requires harmonized protocols, robust environmental compensation models, standardized UAV procedures, shared datasets, and integrated diagnostic frameworks capable of linking thermal anomalies with electrical performance and degradation pathways.

6. Conclusions

This review examined IRTG as a contactless and field-deployable diagnostic method for PV systems, with emphasis on how thermal imaging supports fault localization, performance benchmarking, and maintenance planning at scale. The paper also highlighted how recent progress in UAV deployment and algorithmic automation (image processing, ML, and deep learning) is transforming PV inspection workflows from manual, reactive checks into increasingly data-driven and predictive monitoring pipelines.

A key conclusion is that passive IRTG under natural irradiance remains the most practical thermographic modality for routine outdoor inspections because it can capture temperature anomalies (e.g., hot cells, diode activation, interconnect issues) without system shutdown. At the same time, the literature indicates that thermal anomalies are not merely visual indicators: string-level impacts can be measurable, where affected substrings are a more informative predictor of yield loss than hotspot temperature alone. Reported field analyses show that each module substring containing an anomaly can reduce string output on average (order of ~1% per affected substring), while localized overheating is commonly associated with several-percent energy losses and can contribute to longer-term degradation when persistent. However, it is important to emphasize that thermographic measurements provide indirect indicators of electrical performance rather than direct quantification of I-V degradation. Consequently, IRTG should be regarded primarily as a qualitative or semi-quantitative screening tool, and temperature deviations cannot be universally translated into standardized pass/fail criteria.

Beyond literature synthesis, the Savona Campus experimental campaign reinforced that the quality and interpretability of thermal results depend strongly on measurement geometry and operating conditions. With a bifacial PV bench and fixed camera distance, the study observed distinct thermal responses across morning/noon/afternoon sessions as irradiance and solar incidence evolved, while camera viewing angle influenced the apparent hotspot visibility, particularly when module azimuth aligned more closely with the sun later in the day. This illustrates that even for the same module, the thermal "signature" is not fixed; it is a function of irradiance, incidence angle, and viewing configuration, underscoring the need to document and control these parameters in field protocols.

From the failure-mechanism perspective, the reviewed fault taxonomy (breakage/cracks, delamination, corrosion, hotspot formation, and soiling) supports an important practical point: thermal anomalies often represent a convergence of electrical and material degradation pathways, not isolated events. For instance, hotspots can arise from shading, mismatch, contact defects, cracks, or diode behavior, while delamination and moisture ingress can accelerate metallization/interconnect corrosion and amplify resistive heating. Similarly, soiling is not only an optical loss mechanism; it can create non-uniform irradiance and thermal gradients that complicate diagnosis and may promote hotspot evolution under sustained neglect. The soiling studies summarized in the manuscript further indicate that dust can cause substantial technology-dependent losses (especially for wide bandgap devices), while minor coverage may remain thermally subtle, thus strengthening the argument for combining thermal imaging with RGB/visual confirmation in operational inspections.

When comparing inspection modalities, the overarching finding is that no single technique is sufficient for comprehensive PV diagnostics across all defect types and operational contexts. Visual inspection is fast and economical for surface-visible defects, but it is limited for electrically active, early-stage, or internal faults; EL provides high-resolution insight into microcracks and inactive regions but is operationally constrained; EPIT is powerful at cell-level defect localization under controlled excitation; and IRTG/aIRTG offer scalable, in-field monitoring for thermal signatures, especially when paired with UAV platforms for rapid plant-wide coverage. Consequently, the paper's comparative framing (Table 3) is well aligned with the evidence base: robust diagnostics increasingly depend on multi-method and multi-sensor workflows rather than isolated testing.

A major discussion point emerging from Section 5 is that inspection effectiveness is now tightly coupled to the maturity of inspection algorithms. Digital image processing remains foundational for denoising, enhancement, segmentation, and feature extraction, while ML and CNN-based pipelines enable scalable defect classification and localization across large datasets. However, the critical perspective also shows that algorithmic progress is currently constrained by systemic issues: limited public datasets with reliable annotations, domain shift between lab/ground imagery and UAV-acquired thermograms, and underrepresentation of bifacial-specific thermal behaviors. These gaps directly limit reproducibility, generalization, and real-world transfer of "high-accuracy" models reported under controlled conditions.

From a standards and deployment standpoint, the review identifies a central bottleneck: harmonization of thermographic inspection protocols. Even where IEC guidance structures outdoor IR inspections, the document is instructional and does not provide universal pass/fail severity thresholds, precisely because IRTG does not directly quantify electrical impact in a manner comparable to qualification standards. Field implementations vary substantially (irradiance constraints, wind tolerance, viewing-angle handling, calibration practices), and this procedural variability makes cross-study comparison difficult while limiting the establishment of universally transferable temperature-based severity classifications. In parallel, UAV-based thermography introduces additional uncertainty sources, i.e., altitude, camera pitch/roll, vibration, and atmospheric transmissivity, that are still rarely quantified systematically in PV inspection studies.

Looking forward, the most impactful research and engineering directions suggested by the findings in this manuscript are:

Protocol convergence and uncertainty quantification: Move toward standardized reporting of irradiance, wind, emissivity assumptions, viewing geometry, calibration methods, and uncertainty bounds, particularly for UAV campaigns.

Performance-linked interpretation: Develop generalizable models that connect thermal signatures to electrical impacts (substring/diode behavior, shading dynamics, aging mechanisms), while recognizing that thermography remains complementary to, rather than a substitute for, direct electrical characterization.

Multi-modal diagnostic fusion: Systematically integrate IRTG/aIRTG with RGB context, EL/PL (where feasible), IV/SCADA analytics, and maintenance history to improve fault attribution (e.g., distinguishing soiling-induced hot regions from electrically driven heating).

Algorithm robustness for field variability: Expand datasets and benchmarking to reflect real PV diversity (module technologies, climates, UAV configurations, bifacial operation) and prioritize domain adaptation and physics-informed learning to mitigate domain shift.

In conclusion, the reviewed evidence supports IR thermography—particularly when scaled through UAV platforms and strengthened by modern image-processing and learning algorithms—as a valuable component of contemporary PV inspection. Its principal strengths lie in non-invasive deployment, scalability, and rapid anomaly screening. Its limitations include indirect linkage to electrical degradation, sensitivity to environmental variability, and the absence of universal quantitative severity thresholds. Therefore, thermography delivers its greatest value when integrated within a multi-modal diagnostic framework that combines standardized acquisition, quantified uncertainty, complementary electrical testing, and performance-aware analytics to guide timely maintenance decisions and sustain long-duration, high-yield PV operation.

Funding: This research received no external funding.

Data Availability Statement: The original contributions presented in this study are included in the article. Further inquiries can be directed to the corresponding author.

Acknowledgments: This research is part of the Italian National Program PNRR—Raise PNRR—Ecosistema dell'Innovazione ECS00000035 "RAISE (Robotics and AI for Socio economic Empowerment)"—SPOKE 3 "Environmental Caring and Protection Technologies, towards a Zero Emission Environment"—Task 3.2 "Technologies for energy storage". This research is a part of the Interreg-Alcotra 2021–2027 "Ermess Green" Program. Antonella Priarone (University of Genova) is acknowledged for her guidance and supervision in this research.

Conflicts of Interest: The authors declare no conflict of interest.

Abbreviations

aIRTG	Aerial Infrared Thermography
AI	Artificial Intelligence
AR5	Fifth Assessment Report (IPCC)
BPV	Bifacial Photovoltaic
CCD	Charge-Coupled Device
CNN/CNNs	Convolutional Neural Network(s)
CPU	Central Processing Unit
CIGS	Copper Indium Gallium Selenide
DAQ	Data Acquisition
DC	Direct Current
DIP	Digital Image Processing
DL	Deep Learning
EDX	Energy-Dispersive X-Ray (Spectroscopy)
EL	Electroluminescence
EPIT	Electrical Pulsed Infrared Thermography
EU	European Union
EVA	Ethylene Vinyl Acetate
FFT	Fast Fourier Transform
GPS	Global Positioning System
IEC	International Electrotechnical Commission
IEA	International Energy Agency
IEEE	Institute of Electrical and Electronics Engineers
IR	Infrared
IRTG	Infrared Thermography
IPCC	Intergovernmental Panel on Climate Change
I–V	Current–Voltage (I–V) Curve (I = Current; V = Voltage)
LDA	Linear Discriminant Analysis
LIT	Lock-In Thermography
ML	Machine Learning
NDT	Non-Destructive Testing
NDTT	Non-Destructive Testing Technique
O&M	Operation and Maintenance
PCA	Principal Component Analysis
PID	Potential-Induced Degradation
PL	Photoluminescence
PV	Photovoltaic
QDA	Quadratic Discriminant Analysis
REPowerEU	REPowerEU plan
RGB	Red–Green–Blue (Imaging)
RUV	Resonance Ultrasonic Vibration
SCADA	Supervisory Control and Data Acquisition
SEM	Scanning Electron Microscopy
SHT	Step Heating Thermography
SNR	Signal-to-Noise Ratio
SPIE	Society of Photo-Optical Instrumentation Engineers
SVM	Support Vector Machine
TAT	Title, Abstract, and Topic
TS	Technical Specification
UAV/UAVs	Unmanned Aerial Vehicle(s)
UK	United Kingdom

UV	Ultraviolet
UVF	Ultraviolet Fluorescence
VTM	Visual Testing Method
UniGe	University of Genoa (Università di Genova)
c-Si	Crystalline Silicon

References

1. IEA. *Trends in PV Applications 2023*; International Energy Agency: Paris, France, 2023. Available online: https://iea-pvps.org/trends_reports/trends-2023/ (accessed on 17 September 2025).
2. REN21. *Renewables 2023 Global Status Report*; REN21 Secretariat: Paris, France, 2023. Available online: https://www.ren21.net/gsr-2023/ (accessed on 17 September 2025).
3. Polverini, D.; Espinosa, N.; Eynard, U.; Leccisi, E.; Ardente, F.; Mathieux, F. Assessing the carbon footprint of photovoltaic modules through the EU Ecodesign Directive. *Sol. Energy* **2023**, *257*, 1–9. [CrossRef]
4. Skoczek, A.; Sample, T.; Dunlop, E.D. The results of performance measurements of field-aged crystalline silicon photovoltaic modules. *Prog. Photovolt. Res. Appl.* **2009**, *17*, 227–240. [CrossRef]
5. Fesharaki, V.J.; Dehghani, M.; Fesharaki, J.J.; Tavasoli, H. The effect of temperature on photovoltaic cell efficiency. In Proceedings of the 1st International Conference on Emerging Trends in Energy Conservation—ETEC Tehran, Tehran, Iran, 20–21 November 2011. Available online: https://www.academia.edu/92375607/The_Effect_of_Temperature_on_Photovoltaic_Cell_Efficiency (accessed on 17 September 2025).
6. Ndiaye, A.; Charki, A.; Kobi, A.; Kébé, C.M.F.; Ndiaye, P.A.; Sambou, V. Degradations of silicon photovoltaic modules: A literature review. *Sol. Energy* **2013**, *96*, 140–151. [CrossRef]
7. Huld, T.; Gottschalg, R.; Beyer, H.G.; Topič, M. Mapping the performance of PV modules, effects of module type and data averaging. *Sol. Energy* **2010**, *84*, 324–338. [CrossRef]
8. IEA. International Energy Agency PVPS Task 13: Performance and Reliability of Photovoltaic Systems—Subtask 3.2. In *PVPS Task 13. Review of Failures of Photovoltaic Modules*; Report IEA-PVPS T13-01:2014; IEA: Paris, France, 2014. Available online: https://iea-pvps.org/wp-content/uploads/2020/01/IEA-PVPS_T13-01_2014_Review_of_Failures_of_Photovoltaic_Modules_Final.pdf (accessed on 17 September 2025).
9. Deitsch, S.; Christlein, V.; Berger, S.; Buerhop-Lutz, C.; Maier, A.; Gallwitz, F.; Riess, C. Automatic classification of defective photovoltaic module cells in electroluminescence images. *Sol. Energy* **2019**, *185*, 455–468. [CrossRef]
10. Kandeal, A.W.; Elkadeem, M.R.; Kumar Thakur, A.; Abdelaziz, G.B.; Sathyamurthy, R.; Kabeel, A.E.; Yang, N.; Sharshir, S.W. Infrared thermography-based condition monitoring of solar photovoltaic systems: A mini review of recent advances. *Sol. Energy* **2021**, *223*, 33–43. [CrossRef]
11. Parenti, M.; Fossa, M.; Delucchi, L. A model for energy predictions and diagnostics of large-scale photovoltaic systems based on electric data and thermal imaging of the PV fields. *Renew. Sustain. Energy Rev.* **2024**, *206*, 114858. [CrossRef]
12. Sadeghi, R.; Hejazymehr, E.; Arefnia, M. The impact of shading patterns and enhancement of thermal resistance on energy efficiency in an office building. In Proceedings of the 12th International Conference on Engineering and Technology, Oslo, Norway, 20 June 2019. Available online: https://papers.ssrn.com/sol3/papers.cfm?abstract_id=3693258 (accessed on 15 March 2026).
13. Capozzoli, A.; Fantucci, S.; Favoino, F.; Perino, M. Vacuum Insulation Panels: Analysis of the Thermal Performance of Both Single Panel and Multilayer Boards. *Energies* **2015**, *8*, 2528–2547. [CrossRef]
14. Yuan, J. Impact of Insulation Type and Thickness on the Dynamic Thermal Characteristics of an External Wall Structure. *Sustainability* **2018**, *10*, 2835. [CrossRef]
15. Amani, N. Energy efficiency of residential buildings using thermal insulation of external walls and roof based on simulation analysis. *Energy Storage Sav.* **2025**, *4*, 48–55. [CrossRef]
16. Sadeghi, R.; Amininezhad Kimia, A.; Yarahmadi, D.; Tajik, S. Effect of louvres, overhang, and sidefins shading patterns on energy consumption in an office building. In Proceedings of the International Conference on Engineering and Technology, Oslo, Norway, 27 December 2019.
17. Daffara, C.; Muradore, R.; Piccinelli, N.; Gaburro, N.; de Rubeis, T.; Ambrosini, D. A Cost-Effective System for Aerial 3D Thermography of Buildings. *J. Imaging* **2020**, *6*, 76. [CrossRef] [PubMed]
18. Groesdonk, P.; Kölsch, B.; Schiricke, B.; Diel, M.; Patel, N.; Hoffschmidt, B. Experimental investigation of acoustic airtightness measurement and UAV-based quantitative infrared thermography for building energy performance assessment. *J. Build. Eng.* **2026**, *117*, 114713. [CrossRef]
19. Videras Rodríguez, M.; Gómez Melgar, S.; Andújar Márquez, J.M. Evaluation of aerial thermography for measuring the thermal transmittance (U-value) of a building façade. *Energy Build.* **2024**, *324*, 114874. [CrossRef]

20. Tardy, F. A review of the use of infrared thermography in building envelope thermal property characterization studies. *J. Build. Eng.* **2023**, *75*, 106918. [CrossRef]
21. Henry, C.; Poudel, S.; Lee, S.W.; Jeong, H. Automatic detection system of deteriorated PV modules using drone with thermal camera. *Appl. Sci.* **2020**, *10*, 3802. [CrossRef]
22. Qian, F.; Shi, Z.; Yang, L. AI-Assisted Multidimensional Optimization of Thermal and Morphological Performance in Small-to-Medium Sports Buildings. *Appl. Sci.* **2025**, *15*, 9912. [CrossRef]
23. Buratti, Y.; Javier, G.M.N.; Abdullah-Vetter, Z.; Dwivedi, P.; Hameiri, Z. Machine learning for advanced characterisation of silicon photovoltaics: A comprehensive review of techniques and applications. *Renew. Sustain. Energy Rev.* **2024**, *202*, 114617. [CrossRef]
24. Cuong, T.H. Drone-based thermal imaging system for identifying damaged photovoltaic modules. *Open Access Res. J. Sci. Technol.* **2023**, *7*, 028–033. [CrossRef]
25. *IEC TS 62446-3:2017*; Photovoltaic System Documentation and Inspection—Part 3: Infrared Thermography. IEC: Geneva, Switzerland, 2017. Available online: https://datatec.es/wp-content/uploads/2019/09/Normativa-IEC-TS-62446-3.pdf (accessed on 20 September 2025).
26. Perry, K.; Nguyen, Q.; Jordan, D.; Deline, C.; Putrah, B. *Relating Aerial Infrared Thermography Defects to Photovoltaic Performance: Preprint*; U.S. National Renewable Energy Laborator: Golden, CO, USA, 2024. Available online: https://docs.nrel.gov/docs/fy24osti/90316.pdf (accessed on 20 September 2025).
27. Choi, K.; Suh, J. Fault Detection and Power Loss Assessment for Rooftop Photovoltaics Installed in a University Campus, by Use of UAV-Based Infrared Thermography. *Energies* **2023**, *16*, 4513. [CrossRef]
28. Et-Taleby, A.; Chaibi, Y.; Ayadi, N.; Elkari, B.; Benslimane, M.; Chalh, Z. Enhancing fault detection and classification in photovoltaic systems based on a hybrid approach using fuzzy logic algorithm and thermal image processing. *Sci. Afr.* **2025**, *28*, e02684. [CrossRef]
29. Oliveira, A.K.V.; Aghaei, M.; Madukanya, U.E.; Rüther, R. Fault inspection by aerial infrared thermography in a PV plant after a meteorological tsunami. *Rev. Bras. Energ. Sol.* **2019**, *10*, 17–25. [CrossRef]
30. Jahn, U.; Herz, M.; Köntges, M.; Parlevliet, D.; Paggi, M.; Tsanakas, I.; Stein, J.; Berger, K.A.; Ranta, S.; French, R.; et al. Review on infrared and electroluminescence imaging for PV field applications: IEA-PVPS Task 13, Subtask 3.3. In *Report IEA-PVPS T13-10:2018*; International Energy Agency Photovoltaic Power Systems Programme: Paris, France, 2018. Available online: https://iea-pvps.org/wp-content/uploads/2020/01/Review_on_IR_and_EL_Imaging_for_PV_Field_Applications_by_Task_13.pdf (accessed on 25 September 2025).
31. İmak, A. Automatic classification of defective photovoltaic module cells based on a novel CNN-PCA-SVM deep hybrid model in electroluminescence images. *Turk. J. Sci. Technol.* **2024**, *19*, 497–508. [CrossRef]
32. Kim, D.; Youn, J.; Kim, C. Automatic fault recognition of photovoltaic modules based on statistical analysis of UAV thermography. *Int. Arch. Photogramm. Remote Sens. Spatial Inf. Sci.* **2017**, *42*, 179–182. [CrossRef]
33. Michail, A.; Livera, A.; Tziolis, G.; Carús Candás, J.L.; Fernandez, A.; Antuña Yudego, E.; Fernández Martínez, D.; Antonopoulos, A.; Tripolitsiotis, A.; Partsinevelos, P.; et al. A comprehensive review of unmanned aerial vehicle-based approaches to support photovoltaic plant diagnosis. *Heliyon* **2024**, *10*, e23983. [CrossRef]
34. Carpintero, L.A.; Terrados, C.; González-Francés, D.; Sulca, K.P.; Alonso, V.; González, M.A.; Martínez, O. Martínez, Electroluminescence inspections of PV modules and strings by a self-powering configuration in daylight mode. *Sol. Energy* **2025**, *301*, 113913. [CrossRef]
35. del Prado Santamaría, R.; Dhimish, M.; dos Reis Benatto, G.A.; Kari, T.; Poulsen, P.B.; Spataru, S.V. From Indoor to Daylight Electroluminescence Imaging for PV Module Diagnostics: A Comprehensive Review of Techniques, Challenges, and AI-Driven Advancements. *Micromachines* **2025**, *16*, 437. [CrossRef]
36. Le, P.T.; Nguyen, Q.L. Defect analysis and performance evaluation of photovoltaic modules using quantitative electroluminescence imaging. *Clean Energy* **2025**, *9*, 177–189. [CrossRef]
37. Puppala, H.; Maganti, L.S.; Peddinti, P.R.T.; Motapothula, M.R. Thermographic inspections of solar photovoltaic plants in India using unmanned aerial vehicles: Analysing the gap between theory and practice. *Renew. Energy* **2024**, *237*, 121694. [CrossRef]
38. Bommes, L.; Pickel, T.; Buerhop-Lutz, C.; Hauch, J.; Brabec, C.; Peters, I.M. Computer vision tool for detection, mapping, and fault classification of photovoltaics modules in aerial IR videos. *Prog. Photovolt. Res. Appl.* **2021**, *29*, 1236–1251. [CrossRef]
39. Bommes, L.; Hoffmann, M.; Buerhop-Lutz, C.; Pickel, T.; Hauch, J.; Brabec, C.; Maier, A.; Peters, I.M. Anomaly detection in IR images of PV modules using supervised contrastive learning. *Prog. Photovolt. Res. Appl.* **2022**, *30*, 597–614. [CrossRef]
40. Zhou, Z.; Tkachenko, S.; Bahl, P.; Tavener, D.; de Silva, C.; Timchenko, V.; Jiang, J.Y.; Keevers, M.; Green, M. Passive PV module cooling under free convection through vortex generators. *Renew. Energy* **2022**, *190*, 319–329. [CrossRef]
41. Köntges, M.; Oreski, G.; Jahn, U.; Herz, M.; Hacke, P.; Weiß, K.A. *Assessment of Photovoltaic Module Failures in the Field*; Report IEA-PVPS T13-09:2017; International Energy Agency: Paris, France, 2017. Available online: https://iea-pvps.org/wp-content/uploads/2017/09/170515_IEA-PVPS-report_T13-09-2017_Internetversion_2.pdf (accessed on 27 September 2025).

42. Koester, L.; Lindig, S.; Louwen, A.; Astigarraga, A.; Manzolini, G.; Moser, D. Review of photovoltaic module degradation, field inspection techniques and techno-economic assessment. *Renew. Sustain. Energy Rev.* **2022**, *165*, 112616. [CrossRef]
43. Duffie, J.A.; Beckman, W.A. *Solar Engineering of Thermal Processes*, 4th ed.; Wiley: Hoboken, NJ, USA, 2013. [CrossRef]
44. Tsanakas, J.A.; Ha, L.D.; al Shakarchi, F. Advanced inspection of photovoltaic installations by aerial triangulation and terrestrial georeferencing of thermal/visual imagery. *Renew. Energy* **2017**, *102*, 224–233. [CrossRef]
45. Djordjevic, S.; Parlevliet, D.; Jennings, P. Detectable faults on recently installed solar modules in Western Australia. *Renew. Energy* **2014**, *67*, 215–221. [CrossRef]
46. Winkel, P.; Smretschnig, J.; Wilbert, S.; Röger, M.; Sutter, F.; Blum, N.; Carballo, J.A.; Fernandez, A.; Alonso-García, M.d.C.; Polo, J.; et al. Electrothermal modeling of photovoltaic modules for the detection of hot-spots caused by soiling. *Energies* **2024**, *17*, 4878. [CrossRef]
47. Haque, A.; Bharath, K.V.S.; Khan, M.A.; Khan, I.; Jaffery, Z.A. Fault diagnosis of photovoltaic modules. *Energy Sci. Eng.* **2019**, *7*, 622–644. [CrossRef]
48. del Prado Santamaría, R.; dos Reis Benatto, G.A.; Dhimish, M.; Koc, T.; Friansyah, R.; Kari, T.; Mahmood, A.; Poulsen, P.B.; Spataru, S.V. Influence of irradiance and drone altitude in infrared thermography inspections of photovoltaic plants. *EPJ Photovolt.* **2025**, *16*, 31. [CrossRef]
49. Herraiz, Á.H.; Marugán, A.P.; Márquez, F.P.G. A review on condition monitoring system for solar plants based on thermography. In *Non-Destructive Testing and Condition Monitoring Techniques for Renewable Energy Industrial Assets*; Butterworth-Heinemann: Oxford, UK, 2020; pp. 103–118. [CrossRef]
50. van Eck, N.J.; Waltman, L. Software survey: VOSviewer, a computer program for bibliometric mapping. *Scientometrics* **2010**, *84*, 523–538. [CrossRef]
51. Tsanakas, J.A.; Botsaris, P.N. Passive and active thermographic assessment as a tool for condition-based performance monitoring of photovoltaic modules. *J. Sol. Energy Eng.* **2011**, *133*, 021010. [CrossRef]
52. Lopez, F.; Ibarra-Castanedo, C.; de Paulo Nicolau, V.; Maldague, X. Optimization of pulsed thermography inspection by partial least-squares regression. *NDT E Int.* **2014**, *66*, 128–138. [CrossRef]
53. Sinha, A.; Sastry, O.S.; Gupta, R. Detection and characterisation of delamination in PV modules by active infrared thermography. *Nondestruct. Test. Eval.* **2016**, *31*, 1–16. [CrossRef]
54. Breitenstein, O.; Straube, H.; Iwig, K. Lock-in thermography with depth resolution on silicon solar cells. *Sol. Energy Mater. Sol. Cells* **2018**, *185*, 66–74. [CrossRef]
55. Ostapenko, S.; Dallas, W.; Hess, D.; Polupan, O.; Wohlgemuth, J. Crack detection and analyses using resonance ultrasonic vibrations in crystalline silicon wafers. In Proceedings of the 2006 IEEE 4th World Conference on Photovoltaic Energy Conversion (WCPEC-4), Waikoloa, HI, USA, 7–12 May 2006; Volume 1, pp. 920–923. [CrossRef]
56. Skoplaki, E.; Palyvos, J.A. Operating temperature of photovoltaic modules: A survey of pertinent correlations. *Renew. Energy* **2009**, *34*, 23–29. [CrossRef]
57. Skomedal, Å.F.; Aarseth, B.L.; Haug, H.; Selj, J.; Marstein, E.S. How much power is lost in a hot-spot? A case study quantifying the effect of thermal anomalies in two utility scale PV power plants. *Sol. Energy* **2020**, *211*, 1255–1262. [CrossRef]
58. Simon, M.; Meyer, E.L. Detection and analysis of hot-spot formation in solar cells. *Sol. Energy Mater. Sol. Cells* **2010**, *94*, 106–113. [CrossRef]
59. Glavaš, H.; Vukobratović, M.; Primorac, M.; Muštran, D. Infrared thermography in inspection of photovoltaic panels. In Proceedings of the International Conference on Smart Systems and Technologies (SST 2017), Osijek, Croatia, 18–20 October 2017; pp. 63–68. [CrossRef]
60. Khalil, I.U.; Ul-Haq, A.; Mahmoud, Y.; Jalal, M.; Aamir, M.; Ahsan, M.U.; Mehmood, K. Comparative analysis of photovoltaic faults and performance evaluation of its detection techniques. *IEEE Access* **2020**, *8*, 26676–26700. [CrossRef]
61. IEA-PVPS. Quantification of Technical Risks in PV Power Systems: Task 13 Performance, Operation and Reliability of Photovoltaic Systems—Identify, Analyse, Mitigate. 2021. Available online: https://iea-pvps.org/wp-content/uploads/2021/11/Report-IEA%E2%80%93PVPS-T13-23_2021-Quantification-of-Technical-Risks-in-PV-Power-Systems_final.pdf (accessed on 9 October 2025).
62. Sinclair, K.; Sinclair, M. *Silicon Solar Module Visual Inspection Guide: Catalogue of Defects to Be Used as a Screening Tool*, Version 1.8; Zayed Energy and Ecology Centre: Masdar, Malawi, 2016. Available online: https://www.engineeringforchange.org/wp-content/uploads/2017/09/Solar-PV-Product-Visual-Inspection-Guide.pdf (accessed on 10 October 2025).
63. Wohlgemuth, J.H.; Kurtz, S. Reliability testing beyond qualification as a key component in photovoltaic's progress toward grid parity. In Proceedings of the 2011 IEEE International Reliability Physics Symposium (IRPS), Monterey, CA, USA, 10–14 April 2011; pp. 5B.4.1–5B.4.6. Available online: https://ieeexplore.ieee.org/abstract/document/5784534 (accessed on 9 October 2025).
64. Tongwei. Can Solar Panels Crack from Cold Water. 2024. Available online: https://en.tongwei.cn/blog/131.html (accessed on 17 September 2025).

65. Quintana, M.A.; King, D.L.; McMahon, T.J.; Osterwald, C.R. Commonly observed degradation in field-aged photovoltaic modules. In Proceedings of the 29th IEEE Photovoltaic Specialists Conference (PVSC), New Orleans, LA, USA, 19–24 May 2002; pp. 1436–1439. Available online: https://ieeexplore.ieee.org/abstract/document/1190879 (accessed on 9 October 2025).
66. Xu, H.; Hong, G.; Shao, L.; Xu, F.; Lou, W. Mechanical characteristic of glass–glass photovoltaic module and its wind-induced damage mechanism. *Sol. Energy* **2026**, *306*, 114291. [CrossRef]
67. Nakagawa, K.; Kaligambe, A.; Fujita, G. Comparative analysis of defective solar PV module inspection using thermal infrared and electroluminescence imaging techniques. In Proceedings of the 2023 4th International Conference on High Voltage Engineering and Power Systems (ICHVEPS), Bali, Indonesia, 6–10 August 2023; pp. 98–102. [CrossRef]
68. Gao, H.; Fan, S.; He, M.; Wang, Y.; Hong, W.; Ding, W. CrackNet: A transformer-based approach for detecting microcrack in photovoltaic panels based on electroluminescence images. *Renew. Energy* **2026**, *256*, 124549. [CrossRef]
69. Samrouth, K.; Nazir, S.; Bakir, N.; Khodor, N. Dual CNN for photovoltaic electroluminescence images microcrack detection. *Array* **2025**, *27*, 100442. [CrossRef]
70. Kull, K.; Asad, B.; Khan, M.A.; Naseer, M.U.; Kallaste, A.; Vaimann, T. Faults, failures, reliability, and predictive maintenance of grid-connected solar systems: A comprehensive review. *Appl. Sci.* **2025**, *15*, 11461. [CrossRef]
71. koczek, A.; Sample, T.; Dunlop, E.D.; Ossenbrink, H.A. Electrical performance results from physical stress testing of commercial PV modules to the IEC 61215 test sequence. *Sol. Energy Mater. Sol. Cells* **2008**, *92*, 1593–1604. [CrossRef]
72. Kaplanis, S.; Kaplani, E.; Borza, P.N. PV defects identification through a synergistic set of non-destructive testing (NDT) techniques. *Sensors* **2023**, *23*, 3016. [CrossRef] [PubMed]
73. Köntges, M.; Altmann, S.; Heimberg, T.; Jahn, U.; Berger, K.A. Mean degradation rates in PV systems for various kinds of PV module failures. In *Proceedings of the 32nd European Photovoltaic Solar Energy Conference (EU PVSEC 2016), Munich, Germany, 20–24 June 2016*; WIP Renewable Energie: Amsterdam, The Netherlands, 2016. Available online: https://www.researchgate.net/publication/325344145 (accessed on 10 October 2025).
74. del Pero, C.; Aste, N.; Leonforte, F.; Sfolcini, F. Long-term reliability of photovoltaic c-Si modules—A detailed assessment based on the first Italian BIPV project. *Sol. Energy* **2023**, *264*, 112074. [CrossRef]
75. Jordan, D.C.; Silverman, T.J.; Wohlgemuth, J.H.; Kurtz, S.R.; VanSant, K.T. Photovoltaic failure and degradation modes. *Prog. Photovolt. Res. Appl.* **2017**, *25*, 318–326. [CrossRef]
76. Charles, G.; Elizabeth, J. Hot-spot durability testing of amorphous cells and modules. In *Proceedings of the IEEE Photovoltaic Specialists Conference, Las Vegas, NA, USA, 1 February 1985*; IEEE: New York, NY, USA, 1985. Available online: https://www.scopus.com/pages/publications/0022329752 (accessed on 15 March 2026).
77. Nelson, D.L.; Alex, S. Field failure mechanisms for photovoltaic modules. In Proceedings of the IEEE Photovoltaic Specialists Conference (PVSC), Atlanta, GA, USA, 1981. Available online: https://www.scopus.com/pages/publications/0019652979 (accessed on 15 March 2026).
78. Wohlgemuth, J.H. Reliability testing of PV modules. In Proceedings of the IEEE Photovoltaic Specialists Conference (PVSC), Waikoloa, HI, USA, 1994. Available online: https://www.scopus.com/pages/publications/0028703761 (accessed on 15 March 2026).
79. Herrmann, W.; Wiesner, W.; Vaassen, W. Hot spot investigations on PV modules—New concepts for a test standard and consequences for module design with respect to bypass diodes. In Proceedings of the 26th IEEE Photovoltaic Specialists Conference (PVSC), Anaheim, CA, USA, 29 September–3 October 1997; pp. 1129–1132. [CrossRef]
80. Molenbroek, E.; Waddington, D.W.; Emery, K.A. Hot spot susceptibility and testing of PV modules. In Proceedings of the 22nd IEEE Photovoltaic Specialists Conference (PVSC), Las Vegas, NV, USA, 7–11 October 1991; Volume 1, pp. 547–552. [CrossRef]
81. Ferry, A.; Parenti, M.; Thebault, M.; Ménézo, C.; Fossa, M. Optimal tilt angles for bifacial photovoltaic plants across Europe based on cumulative sky and Typical Meteorological Year data. *Sol. Energy* **2025**, *293*, 113475. [CrossRef]
82. Sadeghi, R.; Parenti, M.; Memme, S.; Fossa, M.; Morchio, S. A Review and Comparative Analysis of Solar Tracking Systems. *Energies* **2025**, *18*, 2553. [CrossRef]
83. Qasem, H.; Betts, T.; Mullejans, H.; AlBusairi, H.; Gottschalg, R. *Dust Effect on PV Modules*; Loughborough University Institutional Repository: Leicestershire, UK, 2011. [CrossRef]
84. Mik, K.; Bugaj, M.; Chaja, P. The evaluation of the snail track affected photovoltaic modules by different methods after 3-year operating in central Poland. *Renew. Energy* **2021**, *163*, 504–516. [CrossRef]
85. Bu, C.; Liu, T.; Li, R.; Shen, R.; Zhao, B.; Tang, Q. Electrical pulsed infrared thermography and supervised learning for PV cells defects detection. *Sol. Energy Mater. Sol. Cells* **2022**, *237*, 111561. [CrossRef]
86. Appiah, A.Y.; Zhang, X.; Ayawli, B.B.K.; Kyeremeh, F. Long short-term memory networks-based automatic feature extraction for photovoltaic array fault diagnosis. *IEEE Access* **2019**, *7*, 30089–30101. [CrossRef]
87. Aziz, F.; Ul Haq, A.; Ahmad, S.; Mahmoud, Y.; Jalal, M.; Ali, U. A novel convolutional neural network-based approach for fault classification in photovoltaic arrays. *IEEE Access* **2020**, *8*, 41889–41904. [CrossRef]

88. Paggi, M.; Berardone, I.; Infuso, A.; Corrado, M. Fatigue degradation and electric recovery in silicon solar cells embedded in photovoltaic modules. *Sci. Rep.* **2014**, *4*, 4506. [CrossRef]
89. Li, X.; Li, W.; Yang, Q.; Yan, W.; Zomaya, A.Y. An unmanned inspection system for multiple defects detection in photovoltaic plants. *IEEE J. Photovolt.* **2020**, *10*, 568–576. [CrossRef]
90. Li, X.; Yang, Q.; Lou, Z.; Yan, W. Deep learning-based module defect analysis for large-scale photovoltaic farms. *IEEE Trans. Energy Convers.* **2019**, *34*, 520–529. [CrossRef]
91. Akram, M.W.; Li, G.; Jin, Y.; Chen, X.; Zhu, C.; Ahmad, A. Automatic detection of photovoltaic module defects in infrared images with isolated and develop-model transfer deep learning. *Sol. Energy* **2020**, *198*, 175–186. [CrossRef]
92. Polymeropoulos, I.; Bezyrgiannidis, S.; Vrochidou, E.; Papakostas, G.A. Enhancing solar plant efficiency: A review of vision-based monitoring and fault detection techniques. *Technologies* **2024**, *12*, 175. [CrossRef]
93. Akram, M.W.; Li, G.; Jin, Y.; Chen, X.; Zhu, C.; Zhao, X.; Khaliq, A.; Faheem, M.; Ahmad, A. CNN-based automatic detection of photovoltaic cell defects in electroluminescence images. *Energy* **2019**, *189*, 116319. [CrossRef]
94. Weinreich, B.; Haas, R.; Zehner, M.; Becker, G. Optimierung thermografischer Fehleranalyseverfahren auf Multi-MW-PV-Kraftwerke. In Proceedings of the 26th PV-Symposium Bad Staff, Bad Staff, Germany, 5–9 September 2011; p. 1.
95. de Oliveira, A.K.V.; Aghaei, M.; Rüther, R. Automatic Inspection of Photovoltaic Power Plants Using Aerial Infrared Thermography: A Review. *Energies* **2022**, *15*, 2055. [CrossRef]
96. Kumar, N.M.; Chopra, S.S.; de Oliveira, A.K.V.; Ahmed, H.; Vaezi, S.; Madukanya, U.E.; Castañón, J.M. Solar PV module technologies. In *Photovoltaic Solar Energy Conversion*; Elsevier: Amsterdam, The Netherlands, 2020; pp. 51–78. [CrossRef]
97. Buerhop, C.; Schlegel, D.; Niess, M.; Vodermayer, C.; Weißmann, R.; Brabec, C.J. Reliability of IR-imaging of PV-plants under operating conditions. *Sol. Energy Mater. Sol. Cells* **2012**, *107*, 154–164. [CrossRef]
98. Álvarez-Tey, G.; García-López, C. Strategy Based on Two Stages for IR Thermographic Inspections of Photovoltaic Plants. *Appl. Sci.* **2022**, *12*, 6331. [CrossRef]
99. Aghaei, M.; de Oliveira, A.K.V.; Rüther, R. Fault Inspection by Aerial Infrared Thermography in a PV Plant after a Meteorological Tsunami. In Proceedings of the VII Congresso Brasileiro de Energia Solar, Gramado, Brazil, 17–20 April 2018. [CrossRef]
100. Aghaei, M. *Novel Methods in Control and Monitoring of Photovoltaic Systems*; Politecnico di Milano: Milan, Italy, 2016. Available online: https://hdl.handle.net/20.500.14242/205692 (accessed on 15 March 2026).
101. Bizzarri, F.; Nitti, S.; Malgaroli, G. The use of drones in the maintenance of photovoltaic fields. *E3S Web Conf.* **2019**, *119*, 00021. [CrossRef]
102. Cioaca, C.; Pop, S.; Boscoianu, E.C.; Boşcoianu, M. Aerial infrared thermography: A scalable procedure for photovoltaics inspections based on efficiency and flexibility. *Appl. Mech. Mater.* **2015**, *772*, 546–551. [CrossRef]
103. Tsanakas, J.A.; Botsaris, P.N. An infrared thermographic approach as a hot-spot detection tool for photovoltaic modules using image histogram and line profile analysis. *Int. J. Cond. Monit.* **2012**, *2*, 22–30. [CrossRef]
104. Oliveira, A.K.V.; Aghaei, M.; Rüther, R. Aerial infrared thermography for low-cost and fast fault detection in utility-scale PV power plants. *Sol. Energy* **2020**, *211*, 712–724. [CrossRef]
105. Balasubramani, G.; Thangavelu, V.; Chinnusamy, M.; Subramaniam, U.; Padmanaban, S.; Mihet-Popa, L. Infrared thermography based defects testing of solar photovoltaic panel with fuzzy rule-based evaluation. *Energies* **2020**, *13*, 1343. [CrossRef]
106. Tanda, G.; Migliazzi, M. Infrared thermography monitoring of solar photovoltaic systems: A comparison between UAV and aircraft remote sensing platforms. *Therm. Sci. Eng. Prog.* **2024**, *48*, 102379. [CrossRef]
107. Quater, P.B.; Grimaccia, F.; Leva, S.; Mussetta, M.; Aghaei, M. Light unmanned aerial vehicles (UAVs) for cooperative inspection of PV plants. *IEEE J. Photovolt.* **2014**, *4*, 1107–1113. [CrossRef]
108. Aghaei, M.; Grimaccia, F.; Gonano, C.A.; Leva, S. Innovative automated control system for PV fields inspection and remote control. *IEEE Trans. Ind. Electron.* **2015**, *62*, 7287–7296. [CrossRef]
109. Coello, J.; Perez, L.; Parral, V.; Gomez, R. Implementation of Aerial Thermography Inspection of PV Modules in the O&M Activities in Large PV Plants. In Proceedings of the 32st European Photovoltaic Solar Energy Conference and Exhibition, Munich, Germany, 20–24 June 2016; pp. 1730–1735.
110. Grimaccia, F.; Aghaei, M.; Mussetta, M.; Leva, S.; Quater, P.B. Planning for PV plant performance monitoring by means of unmanned aerial systems (UAS). *Int. J. Energy Environ. Eng.* **2015**, *6*, 47–54. [CrossRef]
111. Intergovernmental Panel on Climate Change (IPCC). Summary for Policymakers. In *Climate Change 2014: Synthesis Report*; IPCC: Geneva, Switzerland, 2014; pp. 1–30. [CrossRef]
112. Elmokadem, T.; Savkin, A.V.; Stan, O.P.; Muresan, V.; Pop, F. Towards fully autonomous UAVs: A survey. *Sensors* **2021**, *21*, 6223. [CrossRef]
113. Evstatiev, B.; Valov, N.; Gabrovska-Evstatieva, K.; Mladenova, T.; Mihailov, N. Investigation of the accuracy of thermographic inspections of photovoltaic modules. In Proceedings of the IEEE International Symposium for Design and Technology of Electronics Packages (SIITME 2023), Pitesti, Romania, 25–28 October 2023; pp. 59–64. [CrossRef]

114. Hausamann, D.; Zirnig, W.; Schreier, G.; Strobl, P. Monitoring of gas pipelines—A civil UAV application. *Aircr. Eng. Aerosp. Technol.* **2005**, *77*, 352–360. [CrossRef]
115. Platini Reges, J.; Lima Moreira, F.D.; Santos Bezerra, L.D.; Ripardo de Alexandria, A.; Reboucas Filho, P.P. Thermographic image processing application in solar followers. *IEEE Lat. Am. Trans.* **2015**, *13*, 3350–3358. [CrossRef]
116. Zhang, G.; Li, B.; Fu, B.; Li, L.; Liu, G. A comparative image analysis of discrete radial Fourier transforms. *Opt. Lasers Eng.* **2010**, *48*, 1186–1192. [CrossRef]
117. Mastromauro, R.A.; Liserre, M.; Dell'Aquila, A. Control issues in single-stage photovoltaic systems: MPPT, current and voltage control. *IEEE Trans. Ind. Inf.* **2012**, *8*, 241–254. [CrossRef]
118. Petrou, M.; Petrou, C. *Image Processing: The Fundamentals*, 2nd ed.; Wiley: Hoboken, NJ, USA, 2011; pp. 1–794. [CrossRef]
119. O'Mahony, N.; Campbell, S.; Carvalho, A.; Harapanahalli, S.; Hernandez, G.V.; Krpalkova, L.; Riordan, D.; Walsh, J. Deep learning vs. traditional computer vision. In *Advances in Intelligent Systems and Computing*; Springer: Cham, Switzerland, 2020; Volume 943, pp. 128–144. [CrossRef]
120. Junior, C.F.C. *Uso de Descritores Morfológicos e Cinemáticos na Identificação Automática de Comportamentos de Animais de Laboratório*; Universidade Federal de Santa Catarina: Florianópolis, Brazil, 2011.
121. The, S.; Ai, S.; Dalle, I.; Galleria, S. Deep Learning in Neural Networks: An Overview. *arXiv* **2014**, arXiv:1404.7828. [CrossRef]
122. Mehta, S.; Azad, A.P.; Chemmengath, S.A.; Raykar, V.; Kalyanraman, S. DeepSolarEye: Power Loss Prediction and Weakly Supervised Soiling Localization via Fully Convolutional Networks for Solar Panels. In Proceedings of the WACV 2018, Lake Tahoe, NV, USA, 12–15 March 2018.
123. Kamilaris, A.; Prenafeta-Boldú, F.X. Deep learning in agriculture: A survey. *Comput. Electron. Agric.* **2018**, *147*, 70–90. [CrossRef]
124. Malof, J.M.; Bradbury, K.; Collins, L.M.; Newell, R.G. A Deep Convolutional Neural Network and a Random Forest Classifier for Solar Photovoltaic Array Detection in Aerial Imagery. *Int. Conf. Renew. Energy Res. Appl.* **2016**, *5*, 650–654.
125. Le, M.; Van Su, L.; Dang Khoa, N.; Dao, V.D.; Ngoc Hung, V.; Hong Ha Thi, V. Remote anomaly detection and classification of solar photovoltaic modules based on deep neural network. *Sustain. Energy Technol. Assess.* **2021**, *48*, 101545. [CrossRef]
126. *IEC 62446-1:2016*; Photovoltaic (PV) Systems—Requirements for Testing, Documentation and Maintenance—Part 1: Grid Connected PV Systems—Documentation, Commissioning Tests and Inspection. International Electrotechnical Commission: Geneva, Switzerland, 2016. Available online: https://webstore.iec.ch/en/publication/28628 (accessed on 20 October 2025).
127. Aragon, B.; Johansen, K.; Parkes, S.; Malbeteau, Y.; Al-mashharawi, S.; Al-amoudi, T.; Andrade, C.F.; Turner, D.; Lucieer, A.; McCabe, M.F. A Calibration Procedure for Field and UAV-Based Uncooled Thermal Infrared Instruments. *Sensors* **2020**, *20*, 3316. [CrossRef]
128. Photovoltaic System Thermography Dataset. Available online: https://gts.ai/dataset-download/photovoltaic-system-thermography-dataset/?utm_source=chatgpt.com (accessed on 15 November 2025).
129. Pierdicca, R.; Paolanti, M.; Felicetti, A.; Piccinini, F.; Zingaretti, P. Automatic Faults Detection of Photovoltaic Farms: SolAIr, a Deep Learning-Based System for Thermal Images. *Energies* **2020**, *13*, 6496. [CrossRef]
130. Setiawan, E.A.; Fathurrahman, M. Exploring insights on deep learning-based photovoltaic fault detection for monofacial and bifacial modules using thermography. *Int. J. Cogn. Comput. Eng.* **2025**, *6*, 495–507. [CrossRef]
131. Mayer, Z.; Epperlein, A.; Vollmer, E.; Volk, R.; Schultmann, F. Investigating the Quality of UAV-Based Images for the Thermographic Analysis of Buildings. *Remote Sens.* **2023**, *15*, 301. [CrossRef]
132. Morando, L.; Recchiuto, C.T.; Calla, J.; Scuteri, P.; Sgorbissa, A. Thermal and Visual Tracking of Photovoltaic Plants for Autonomous UAV Inspection. *Drones* **2022**, *6*, 347. [CrossRef]